

2003-24

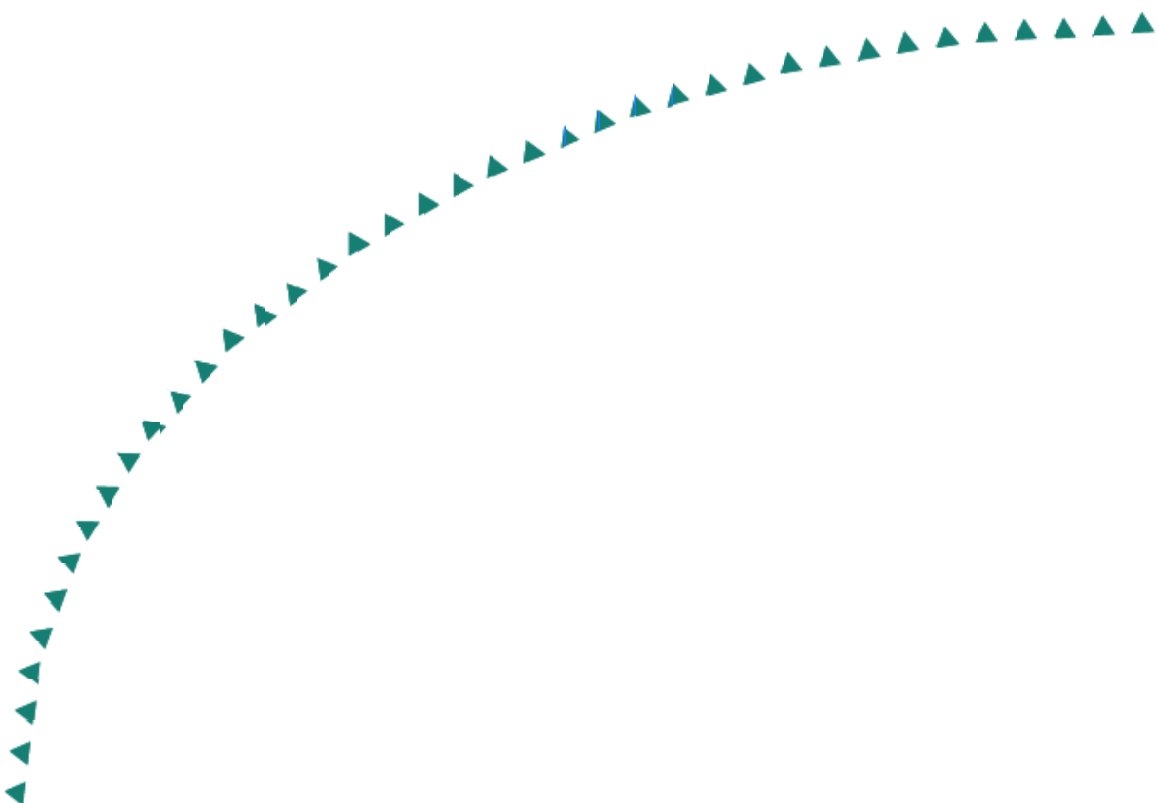
Final Report

# Evaluation of Asphalt Binders Used for Emulsions



**Minnesota Local  
Road Research  
Board**

# Research



## Technical Report Documentation Page

1. Report No. MN/RC – 2003-24	2.	3. Recipients Accession No.	
4. Title and Subtitle <b>EVALUATION OF ASPHALT BINDERS USED FOR EMULSIONS</b>		5. Report Date August 2003	
		6.	
7. Author(s) Timothy R. Clyne, Mihai O. Marasteanu, Arindam Basu		8. Performing Organization Report No.	
9. Performing Organization Name and Address University of Minnesota Department of Civil Engineering 500 Pillsbury Dr. S.E. Minneapolis, MN 55455-0116		10. Project/Task/Work Unit No.	
		11. Contract (C) or Grant (G) No. (c) 81655 (wo) 18	
12. Sponsoring Organization Name and Address Minnesota Department of Transportation Office of Research Services 395 John Ireland Boulevard Mail Stop 330 St. Paul, Minnesota 55155		13. Type of Report and Period Covered Final Report 2001-2003	
		14. Sponsoring Agency Code	
15. Supplementary Notes <a href="http://www.lrrb.gen.mn.us/PDF/200324.pdf">http://www.lrrb.gen.mn.us/PDF/200324.pdf</a>			
16. Abstract (Limit: 200 words) <p>This project was an effort to better characterize asphalt emulsions that are typically used in cold in-place recycling (CIR) applications. A simple approach was presented that treated the cured residue as asphalt binder and applied the standard Superpave specifications to the material. A literature review examined methods that have historically been used to produce, characterize, and apply asphalt emulsions.</p> <p>Four emulsions were tested in this project: CRS-2P, CSS-1, EE, and HFMS-2P. The emulsions were cured two ways, the first being allowed to sit overnight in a pan at room temperature, and the second being a modified RTFOT approach. Air cured samples were also aged in the PAV. These residues were then tested with the BBR and DT at low temperatures and with the DSR at high and intermediate temperatures.</p> <p>AASHTO MP1 specifications were applied in order to characterize the emulsions by PG grade. Following this, AASHTO MP1a specifications were followed in order to find the critical cracking temperature of the emulsions. Master curves were constructed from the DSR tests of complex shear modulus vs. frequency. Finally, a sample mix design was presented using these emulsions and an empirical equation to predict the dynamic modulus of the mixture.</p>			
17. Document Analysis/Descriptors Asphalt Binder Testing                      Emulsion Curing		18. Availability Statement No restrictions. Document available from: National Technical Information Services, Springfield, Virginia 22161	
19. Security Class (this report) Unclassified	20. Security Class (this page) Unclassified	21. No. of Pages 62	22. Price

# **EVALUATION OF ASPHALT BINDERS USED FOR EMULSIONS**

## **Final Report**

Prepared by:

Timothy R. Clyne  
Mihai O. Marasteanu  
Arindam Basu

University of Minnesota  
Department of Civil Engineering  
500 Pillsbury Dr. S.E.  
Minneapolis, MN 55455-0116

**August 2003**

Prepared for:

Minnesota Department of Transportation  
Office of Research Services  
Mail Stop 330  
395 John Ireland Boulevard  
St. Paul, Minnesota 55155-1899

This report represents the results of research conducted by the authors and does not necessarily represent the views or policy of the Minnesota Department of Transportation and/or the Center for Transportation Studies. This report does not contain a standard or specified technique.

## **ACKNOWLEDGEMENTS**

The authors would like to thank the following people for their contributions to this project: Local Road Research Board for providing funds for this project, Dale Bohn at Koch Pavement Solutions for supplying the asphalt emulsions, and Jerry Geib at the Minnesota Department of Transportation for his technical assistance throughout the project.

# TABLE OF CONTENTS

<b>Chapter 1 Introduction</b> .....	1
Background.....	1
Objectives .....	1
Scope.....	1
Organization of the Report.....	2
<b>Chapter 2 Literature Review</b> .....	3
Introduction.....	3
Background.....	3
Asphalt Emulsion Characterization .....	4
Emulsion Residue Recovery.....	4
Conventional Tests for the Characterization of Asphalt Emulsions.....	5
New Methods for Asphalt Emulsion Characterization .....	6
Pre-SHRP Study .....	6
Specification for Surface-Grade Materials .....	6
Analysis by Rotational Viscometry .....	7
Other Recent Development in Asphalt Emulsion Characterization .....	8
Cold In-Place Recycling (CIR).....	9
Performance Based Mix Design for CIR.....	10
Case Study: Using Emulsion Mixes to Minimize Frost Heave .....	10
Summary of Literature Review.....	11
<b>Chapter 3 Research Methodology</b> .....	13
Introduction.....	13
Materials .....	13
Equipment.....	13
Curing .....	13
Testing Procedures.....	14
Bending Beam Rheometer .....	15

Direct Tension.....	16
Dynamic Shear Rheometer .....	16
Additional Tests .....	17
<b>Chapter 4 Results and Discussion .....</b>	<b>19</b>
Introduction.....	19
Performance Grade Analysis .....	19
Dynamic Shear Rheometer .....	19
Bending Beam Rheometer .....	21
PG Grading .....	21
Direct Tension.....	22
AASHTO MP1a Analysis.....	24
Thermal Stress Calculations .....	24
DSR Master Curves .....	28
Phase Angle Master Curves .....	34
Temperature Master Curves at 10 rad/s.....	39
Example CIR Mix Design.....	41
Viscosity Determination .....	41
Witczak Predictive Equation.....	42
Mixture Master Curves .....	45
<b>Chapter 5 Results and Recommendations.....</b>	<b>49</b>
Results.....	49
Recommendations.....	50
<b>References .....</b>	<b>51</b>

## LIST OF TABLES

Table 3.1. Testing Matrix.....	14
Table 3.2. DSR Test Temperatures.....	16
Table 4.1. DSR Results @ 10 rad/s, High Temperature.....	20
Table 4.2. DSR Results @ 10 rad/s, Intermediate Temperature.....	20
Table 4.3. Bending Beam Rheometer Results .....	22
Table 4.4. Asphalt Emulsion Residue “Performance Grades” .....	22
Table 4.5. Direct Tension Test Results .....	23
Table 4.6. Critical Cracking Temperature .....	27
Table 4.7. CAM Model Parameters (Air) .....	29
Table 4.8. CAM Model Parameters (RTFOT).....	29
Table 4.9. CAM Model Parameters (PAV) .....	29
Table 4.10. Calculated Viscosity Values for Emulsions.....	42
Table 4.11. CIR Mix Design Parameters .....	43
Table 4.12. Predicted Dynamic Modulus, CRS-2P .....	44
Table 4.13. Predicted Dynamic Modulus, CSS-1 .....	44
Table 4.14. Predicted Dynamic Modulus, EE.....	44
Table 4.15. Predicted Dynamic Modulus, HFMS-2P .....	44
Table 4.16. Mixture Model Parameters .....	46

## LIST OF FIGURES

Figure 4.1. Thermal Stress, Strength vs. Temperature (CRS-2P PAV).....	25
Figure 4.2. Thermal Stress, Strength vs. Temperature (CSS-1 PAV) .....	26
Figure 4.3. Thermal Stress, Strength vs. Temperature (EE PAV).....	26
Figure 4.4. Thermal Stress, Strength vs. Temperature (HFMS-2P PAV) .....	27
Figure 4.5. DSR Stiffness Master Curve, CRS-2P .....	30
Figure 4.6. DSR Stiffness Master Curve, CSS-1 .....	31
Figure 4.7. DSR Stiffness Master Curve, EE.....	31
Figure 4.8. DSR Stiffness Master Curve, HFMS-2P .....	32
Figure 4.9. DSR Stiffness Master Curve, Air cured residue.....	33
Figure 4.10. DSR Stiffness Master Curve, RTFOT cured residue .....	33
Figure 4.11. DSR Stiffness Master Curve, PAV aged residue .....	34
Figure 4.12. DSR Phase Angle Master Curve, CRS-2P .....	35
Figure 4.13. DSR Phase Angle Master Curve, CSS-1 .....	35
Figure 4.14. DSR Phase Angle Master Curve, EE .....	36
Figure 4.15. DSR Phase Angle Master Curve, HFMS-2P.....	36
Figure 4.16. DSR Phase Angle Master Curve, Air cured residue.....	37
Figure 4.17. DSR Phase Angle Master Curve, RTFOT cured residue .....	38
Figure 4.18. DSR Phase Angle Master Curve, PAV aged residue .....	38
Figure 4.19. $ G^* $ vs. Temperature @ 10 rad/s, Air cured residue .....	39
Figure 4.20. $ G^* $ vs. Temperature @ 10 rad/s, RTFOT cured residue .....	40
Figure 4.21. $ G^* $ vs. Temperature @ 10 rad/s, PAV aged residue .....	40
Figure 4.22. Viscosity vs. Temperature, Air cured residues.....	42
Figure 4.23. Mixture Master Curves ( $ E^* $ vs. Frequency) from Witczak Equation .....	46
Figure 4.24. Mixture Master Curves ( $ E^* $ vs. Temperature) from Witczak Equation .....	47
Figure 4.25. $ E^* $ vs. Frequency, Emulsions and Cell 34 .....	48
Figure 4.26. $ E^* $ vs. Temperature, Emulsions and Cell 34.....	48



## EXECUTIVE SUMMARY

Much emphasis has been placed on pavement preservation in recent years. One of the strategies available for pavement preservation is cold in-place recycling (CIR), which uses asphalt emulsion as a main component. Unlike asphalt binders for which performance-based specifications are readily available, asphalt emulsions lack a similar set of testing procedures. This research effort explored the existent methods used to characterize asphalt emulsions and identified potential test methods for characterizing asphalt emulsions in terms of their field performance. The main objectives of this project were to better understand the role of asphalt emulsions in recycled asphalt pavements and to develop the means to better characterize their properties related to their field performance.

Four different asphalt emulsions were evaluated in this study: CRS-2P, CSS-1, EE (a proprietary engineered emulsion by Koch Pavement Solutions), and HFMS-2P. The emulsions were cured using two methods: in the first method the sample was cured in air in a pan at room temperature, and in the second method the samples were cured in the rolling thin-film oven (RTFOT) apparatus. The air-cured samples were also aged in the pressurized aging vessel (PAV). These residues were then tested with the bending beam rheometer (BBR) and direct tension tester (DTT) at low temperatures and with the dynamic shear rheometer (DSR) at high and intermediate temperatures.

AASHTO MP1 specifications were applied in order to characterize the emulsions by PG grade, shown in the table below. Following this, AASHTO MP1a specifications were followed in order to find the critical cracking temperature,  $T_{cr}$ , of the emulsions. Master curves were constructed from the DSR tests of complex shear modulus vs. frequency. Finally, a sample mix design was presented using these emulsions and an empirical equation to predict the dynamic modulus of the mixture.

<b>Emulsion</b>	<b>Performance Grade</b>
CRS-2P	58-34
CSS-1	52-28
EE	46-34
HFMS-2P	52-34

Based on this research, the air-curing method of recovering asphalt emulsion residue was found to produce more conservative results and it is further recommended as the curing method of choice. MP1 specifications provided a straightforward approach to characterizing the emulsion residues. MP1a analysis, however, showed that the critical cracking temperature,  $T_{cr}$ , obtained by the intersection of thermal stress and strength curves was substantially higher than the limiting temperatures obtained in MP1 specification. More research is needed to determine the reasons for the low DTT strength values for these emulsions, the main factor responsible for the high  $T_{cr}$  results obtained. The CAM model was used to generate master curves of the dynamic shear modulus and phase angle data obtained using the DSR. With the exception of the data at 34°C for EE air, the data could be shifted to form smooth master curves. The phase angle master curves were less smooth indicating most probably the presence of small phase transitions or thixotropy effects, especially in the polymer modified samples. A theoretical CIR mix design was presented using viscosity values calculated from DSR test results and volumetric data gleaned from the literature. A comparison to a conventional dense-graded Superpave mixture showed that the Superpave mixture was significantly stiffer than the mixtures containing asphalt emulsions.

Recommendations for further study include comparing the test results on the emulsion residues obtained in this study to test results of mixtures prepared in the laboratory. This comparison should ultimately incorporate field data to determine if the analysis methods used in this project are reasonably accurate to predict the field performance of CIR asphalt emulsions.

# CHAPTER 1

## INTRODUCTION

### **Background**

Much emphasis has been placed on pavement preservation in the recent years. One of the strategies available for pavement preservation is cold in-place recycling (CIR), in which asphalt emulsions are combined with the recycled asphalt pavement to improve its performance. Unlike the conventional asphalt binders for which performance-based specifications are available, asphalt emulsions do not have performance-based specifications. This research effort explored the existent methods used to characterize asphalt emulsions in order to identify potential test methods for characterizing asphalt emulsions in terms of their field performance.

### **Objectives**

The main objective of this project was to develop a method to determine asphalt emulsions properties that can be related to field performance and based on it to better understand the role of asphalt emulsions in recycled asphalt pavements, with emphasis on CIR applications.

### **Scope**

A literature review was conducted on asphalt emulsion characterization and field application with emphasis on CIR applications. Four different asphalt emulsions, commonly used in Minnesota, were evaluated in this study. Three of them are commonly used in CIR applications, CSS-1, EE (a proprietary engineered emulsion), and HFMS-2. The fourth one, CRS-2P, is used in seal coat applications and was included in the analysis for comparison purposes. The emulsions were cured by two different methods, and the residues were tested following the Superpave specifications: bending beam rheometer (BBR) and direct tension (DTT) were performed at low temperatures and dynamic shear rheometer (DSR) tests were performed at high and intermediate temperatures. Similar test protocols for specifying asphalt emulsions were proposed.

The research proposed should be considered as a first step in the much larger effort to relate asphalt emulsion properties to field performance and should not be considered as a

substitute for all the other factors that ultimately affect the field performance of CIR applications.

### **Organization of the Report**

This report is arranged into five sections: Introduction, Literature Review, Research Methodology, Results and Discussion, and Conclusions and Recommendations. The Literature Review summarizes current methods of curing and testing asphalt emulsions as well as field applications, especially for cold in-place recycling. Research Methodology gives details about the materials and equipment used, along with a description of the physical characterization tests performed in the laboratory. Results and Discussion analyzes the experimental data obtained. The data analysis includes characterizing asphalt emulsions based on PG grading, calculating the newly proposed MP1a critical cracking temperature, constructing master curves from DSR data, and performing a mixture design using empirical predictive equations. The report closes with some final conclusions and recommendations. Literature sources used as supporting materials are cited in the references.

# **CHAPTER 2**

## **LITERATURE REVIEW**

### **Introduction**

In the past years the pavements industry has experienced an increasing use of asphalt emulsions for various applications ranging from surface treatments to full depth reclamation projects. This has led to an increased effort to develop new test methods to better characterize the emulsions and the relation between their properties and the performance of their applications. This literature search reviews the current practice and new developments in the field of asphalt emulsions with particular emphasis on the physical characterization of emulsion residue and the relationship to field performance. Although the main objective of this research focuses on cold in-place recycling (CIR) applications, other asphalt emulsion applications will be briefly discussed in an effort to identify other methods or design principles that have the potential to be applied to CIR.

### **Background**

Asphalt emulsions are constituted of asphalt globules dispersed in a colloidal form in a mixture of water and an emulsifying agent. The emulsifying agent also acts as a stabilizing agent under certain circumstances [1]. The basic idea behind emulsified asphalt is to have a dispersion that is stable under storage, mixing and pumping but breaks down quickly upon contact with aggregates to form an asphalt mixture similar to hot mix asphalt (HMA).

Asphalt emulsions are typically classified based on particle charge and setting properties. The emulsions currently used are either anionic or cationic, although there are some limited applications of non-ionic emulsions. The ionic emulsions take advantage of the fact that most aggregates have a surface charge, thus making an emulsion of the opposite charge most suitable for fast and effective binding; however, for CIR this is not an issue. In general, emulsions are manufactured to have three different setting properties; rapid setting (RS), medium setting (MS) and slow setting (SS). RS and MS emulsions are principally used in applications where the pavement has to reopen to traffic within a very short time after construction. In the case of CIR

applications however, the prevalent requirements are eliminating the moisture and obtaining the desired compaction level, which may require additional amounts of time.

### **Asphalt Emulsion Characterization**

A variety of laboratory tests are conventionally performed on the asphalt emulsions and their residue. In order to obtain properties that can be related to field performance it is of critical importance to obtain an emulsion residue that is representative of the emulsion used in the field. That is why the method of recovery of the asphalt binder from the colloidal mix plays a very important role in any attempt to relate the residue properties to performance.

#### *Emulsion Residue Recovery*

The high temperature distillation procedures that are part of the ASTM standards require the specimen to be heated to 177°C or 260°C. The only exception is the vacuum distillation procedure (ASTM D-6014, 2001) that does not use temperatures higher than 160°C. Recently Takamura [2] showed that such high temperatures can significantly alter or damage the microscopic structure of the emulsion and therefore the residues recovered by these processes do not represent the field conditions where construction is done in ambient temperatures.

He proposed a new residue recovery procedure that uses airflow under ambient temperatures to aptly simulate field conditions. An accelerated mechanism was also proposed for use by quality control labs. The formation of a latex polymer morphology was also explained by optical and electron microscopy. The SEM (Scanning Electron Microscopy) images showed that under field conditions, the SBR latex of an emulsion of polymer modified asphalt remains in the aqueous phase and transforms upon curing to form a continuous microscopic film surrounding the asphalt particles. The forced air-drying procedure, wherein the emulsion was dried under ambient temperatures for 5-6 hours, was found to preserve the microscopic polymer network in the residue. This network was stable at temperatures as high as 180°C. Therefore, this procedure can be said to be the closest laboratory simulation of application conditions. The forced airflow drying procedure can be modified for a rapid recovery of samples by drying in the rolling thin film oven (RTFOT) apparatus for 75 minutes at 85°C. This leaves the microscopic polymer network intact. However, not all emulsions, especially CRS-2P, have similar drying characteristics, and should be safeguarded against laboratory hazards.

### *Conventional Tests for the Characterization of Asphalt Emulsions*

Most of the tests are standardized in AASHTO T 59 and ASTM D 244. A summary of all the standard tests and as well as a set of non-standardized tests can be found in Asphalt Institute's MS-19, Chapter 4 [1].

In general the viscosity is conducted using the Saybolt-Furol apparatus [1]. Two testing temperatures (25°C and 50°C) are used to represent the normal working range of temperatures in the field. A number of tests deal with specific emulsion properties [1], e.g. the *particle charge test* to identify cationic emulsions, the *demulsibility* test to check the speed of breaking of a RS emulsion upon spreading on soil or aggregates, the *sieve test* to quantify the amount of large and unmanageable globules and the test for *miscibility with water* for MS and SS emulsions.

*Storage stability* is a test to determine the ability of an asphalt emulsion to remain as a uniform dispersion [1]. A representative sample is taken in two cylinders and allowed to stand under laboratory temperatures for 24 hours. Samples are then taken from the top and bottom of the cylinders and placed in an oven for a set time. The storage stability is expressed as the numerical difference in the average percentage of residue in the top and bottom samples. Similarly, the *settlement* test is also a measure of the emulsion's stability in storage [1]. A specified volume of the emulsion is allowed to stand in a graduated cylinder for usually 5 days. Small samples are then taken from the top and bottom parts, weighed and heated till the water evaporates. The weights obtained after evaporation are used to find the difference between the asphalt cement contents of the upper and lower portions. Another test identifies the *coating ability and water resistance* of MS emulsions [1]. This test determines the ability of the emulsion to coat the aggregates thoroughly, withstand mixing action while present as a film on the aggregates and withstand the washing action of water. The aggregate is mixed with calcium carbonate dust and then with the emulsion to be tested. The test is conducted mostly for qualitative inspections only.

Other tests are used mainly in quality and process control in the field [1]. These tests include the Field Coating test, the Weight per gallon and the specific gravity. Another test not currently specified in AASHTO and ASTM is the Zeta potential test [1]. It measures the stability of the colloid system with a laboratory device called the zeta-meter. The measurements provide an indication of the setting characteristics.

## *New Methods for Asphalt Emulsion Characterization*

The increased interest in the variety of applications of asphalt emulsions has led to many new research efforts. Some of these new developments in the area of asphalt emulsions characterization, with potential for CIR application, are presented below.

### Pre-SHRP Study

King et al [3] presented some early indications about the performance of emulsions made using polymer-modified asphalts. The tests were limited to (anionic) HF emulsions and a (cationic) CRS emulsion for both neat and polymer modified asphalts. The asphalts were recovered from the respective emulsions by distillation at 204°C, as per ASTM Method D 244. It was found that the use of polymer-modified binder with a HF (High Float) emulsifier could decrease the limiting stiffness temperature by 3°C, i.e. half a PG grade. The study was based on the initial limiting values for S and *m*-values of 200 MPa and 0.35 respectively. It was found that polymer modification had a more significant effect on the *m*-value than on the stiffness. At intermediate temperatures, the critical temperature was defined as that at which the  $|G^*|\sin\delta$  value reached 3000 kPa. Under this criterion, the polymer-modified residues reach the critical temperature about 3°C below those for unmodified residues. However, HF emulsions reached the critical  $|G^*|\sin\delta$  value at temperatures about 1.5°C above the cationic emulsions. At high temperatures, polymer modification was found to improve the binder grade by one grade and by two grades when coupled with the HF emulsifier.

### Specification for Surface-Grade Materials

A similar approach was pursued in evaluating asphalt emulsions used for surface treatments and a new specification for surface applications has been proposed from an extension of the above study [4]. This SPG (Surface Performance Grading) system follows the PG system with certain changes in the DSR high temperature test and BBR test specification limits. The authors proposed that emulsion residues could be efficiently obtained without degrading polymer morphology by a stirred-can procedure performed under a nitrogen blanket at 163°C for 170 minutes. A survey by TxDOT found that aggregate loss due to flow and brittle fracture at high and low temperatures respectively were the principle modes of distress for surface treatments. Fatigue at intermediate temperatures was not observed for surface treatments. Moreover, the



distresses occurred mostly after one year in service. Field aging conditions after one year could be simulated in the laboratory by subjecting the original residue to PAV aging only. The SPG system proposes the following new binder specification limits:

1. Minimum  $|G^*|/\sin\delta$  at 10rad/s at high performance temperature = 0.75 kPa
2. Maximum  $S = 500$  MPa and minimum  $m$ -value = 0.24 at 8 seconds at the low performance temperature. The 10°C offsetting is not used here.

The proposed specification has to be validated from field results.

### Analysis by Rotational Viscometry

The conventional practice for determining the viscosity of emulsions is based on measurements performed with the Saybolt-Furol viscometer. In this test the time taken by a particular volume of the sample to flow through an orifice is measured. From an industrial and a process control standpoint, this test is limited in terms of turnover due to the inherent processes of sample sizing, conditioning and cleanup. It also offers limited process control and most importantly, critical emulsion flow properties cannot be ascertained by this test.

This warranted the use of a Brookfield rotational viscometer. The test has a better repeatability (lower than the 9.6% specified for the Saybolt-Furol viscometer test), a lower analysis time and reduced cleanup time, thereby yielding a 40% increase in turnover. In addition, the thixotropy of the emulsions could be observed at different shear rates. A study performed by Salomon resulted in the following conclusions [5]:

- The rate of change of viscosity was higher for higher shear rates.
- At a sufficiently high shear rate, the emulsion viscosity ultimately reaches a steady state. The primary manifestation of this observation is that if a sufficiently high shear rate is applied, the emulsion viscosity should be able to attain this steady state fairly soon. So, a sample can be initially subjected to a high shear rate and then the shear rate can be decreased once steady state is reached and viscosity measurements can be taken.
- The log (shear stress) vs. log (shear rate) plot as a straight line. The slope of this plot yields the Shear Rate Index, which serves as the parameter that is to be calculated for shear thinning fluids like asphalt emulsions.
- For certain emulsions such as CMS-2, which behave like Newtonian fluids, the Shear Rate Index is close to unity.

### *Other Recent Development in Asphalt Emulsion Characterization*

Deneuvillers et al [6] studied a series of emulsions with different particle size diameters (PSD) and correlated the various rheological properties like viscosity, breaking index, cohesion build-up, etc. with respect to parameters like median diameter of the emulsion gel particles and their standard deviation, and also arrived at characterizing grading curves. ( $SD = 0.5\log(D_{84\%}/D_{16\%})$ ; D = Median diameter at which the subscripted volume of particles pass the sieve.) For a given type of emulsion (setting characteristic) the breaking index decreases as the median diameter increases, primarily due to a decrease in the specific surface area and a lower requirement of filler to break the emulsion. Moreover, the viscosity of a given emulsion increases as the standard deviation decreases. These characteristics were correlated with field performance with a setup similar to the SCREG apparatus mentioned before. The field tests showed that the rate of cohesion build-up got faster as the standard deviation and the median diameter decreased. For a given chemical composition, the rate of cohesion build-up was faster for surface dressings made with emulsions having large specific surface areas. i.e. smaller median diameters.

Le Bec et al [7] formulated an accelerated curing mechanism for cold mixes in laboratory conditions, with the idea of being able to predict final mechanical properties. During laying, the compaction phase facilitates the coalescence of bitumen droplets with a sharp reduction in the moisture and air content of the bulk material. However, a certain amount of water remains in the mix and might take weeks or even months to evaporate. Laboratory tests involve the determination of mechanical properties of the mixture in the shortest possible time. The study shows that conditioning of the test pieces at 50°C and 10% RH gives the same level of (compressive) resistance after five days that would otherwise be obtained in thirty days for test pieces conditioned at 18°C and 50% RH. The results also show that regardless of the temperature and RH conditions, it is almost impossible to completely eliminate the water.

The Gyrotory shear compactor (SGC, in the US), equipped with a water sucking and measuring device, was shown by Lesueur [8] to be a powerful tool for predicting the in place compactibility of cold mixes. Overall water content has no effect on compactibility, but only influences the number of cycles to the onset of water drainage. This is analogous to the field condition when compaction stops when water starts to flow at the surface of the mix. Some laboratory studies were conducted on slab compacted samples but the results and rankings did

not agree with field compactions. In a parallel study, the emulsion-aggregate interactions were studied by an analysis of the water that was drained and collected from the Gyratory shear compactor. The pH of the drained water was always a unit higher than the pH measured by the pH-increase test, amounting to a dilution factor of 10. The pH is not affected by the overall water content, which, when increased, only yielded a lesser ion content due to dilution effects. Electron microscopy showed that breaking starts with a clustering of the emulsion droplets. This phenomenon is enhanced by low surfactant contents.

### **Cold In-Place Recycling (CIR)**

Cold In-Place Recycling (CIR) is one of the methods for recycling asphalt pavement materials. This process consists of mixing a recycled crushed asphalt pavement, a recycling agent and water [9]. Asphalt emulsions play a significant role due to their applicability at normal temperatures. CIR can be done in two ways: full depth and partial depth. In full-depth recycling, both the asphalt layer and portions of the unbound layers are crushed, mixed with binder and placed as a stabilized base course. In partial-depth recycling, only a portion of the asphalt part of the pavement is used, typically between 2 to 4 in, to produce a base course for low-to-medium traffic volume highways.

According to a previous MnDOT study by Newcomb [9] material evaluation is the most important aspect of CIR and governs the performance of the rebuilt pavement to a great extent. The RAP (recycled asphalt pavement) is characterized in terms of moisture content, source gradation (by ignition oven), asphalt content, rutting factor and the PG grading of the recovered asphalt. Some of the important conclusions of this CIR study are as follows:

- RAP gradations have a very high variability.
- Similar results are obtained for source gradation with the ignition oven test or the chemical extraction test.
- The total emulsion demand is a function of the RAP asphalt content.
- HFMS-2p gives the lowest air voids.
- Air voids decrease with an increase in emulsion content.
- Additional curing or compaction beyond the norm does not influence the indirect tensile strength.

- Weather conditions during construction play a key role in the subsequent curing and performance of the recycled pavement.

#### *Performance Based Mix Design for CIR*

A study conducted by Brayton et al [10] evaluated the current Marshall mix design as recommended by AASHTO task Force no. 38 for partial-depth CIR applications and subsequently proposed a Superpave Gyratory Compactor based mix design. The Modified Marshall mix design procedure was identified to have some serious handicaps with respect to laboratory work and field validation. The test is very lengthy, the specimens use less material than suggested, and do not give specifications for some key aspects like curing time, emulsion heating time, parameters for introduction of new aggregates or how to determine optimum emulsion content (OEC) or optimum water content. The procedure also does not accurately simulate field results. Based on their experiments, the authors [10] developed the following specimen preparation specification for the modified Superpave (volumetric) mix-design:

1. The specimens should be cured, after compaction, for 24 hours at 60°C.
2. A minimum of four emulsion contents should be used.
3. The number of gyrations used during compaction should be adjusted to achieve densities similar to field densities.

#### *Case Study: Using Emulsion Mixes to Minimize Frost Heave*

Most of the Canadian pavements are exposed to severe cold weather conditions. The standard pavement structure in Canada consists of multi-layered materials laid onto a mostly heterogeneous roadbed soil. The major form of distress is due to frost heave in the upper layers of the pavement. Certain frost-susceptible soils also undergo differential frost heave, resulting in distortion and cracking of the upper layers. Emulsion mixes were used [11] as base layer in lieu of HMA to successfully reduce this phenomenon of distress. The supporting idea for the project was that laboratory and field observations verified that emulsion mixes have more membrane-like mechanical properties rather than the slab-like properties of HMA. This allows the upper layers of the pavement to follow the roadbed soil movement without cracking. Emulsion mixes are also not susceptible to thermal cracking unlike HMA mixtures. It should also be noted here that the emulsion mixes are more resistant to thermal cracking due to their higher voids content

(12-15%) and lower stiffness. The phenomenon of premature oxidation of binder associated with HMA is also absent for emulsion mixtures.

The project involved the design and rehabilitative construction of a highway segment of an AADT of 1500-2000 with about 5% commercial vehicles. The pavement rehabilitation strategy included a grading correction of the in-situ granular material and the placement of an Emulsion Stabilized Granular Material (ESGM) base followed by an Open Graded Emulsion Mix (OGEM) slurry seal. These strategies were selected in keeping with the criteria outlined for attaining maximum flexibility of the pavement materials under frost heave, maximum resistance to thermal cracking, maximum increase in pavement strength and minimum increase in elevation. The granular correction was done with 33% 19mm clear stone to enable the base granular material to fall inside the gradation envelope under Canadian specifications. The mix design, albeit considering Marshall Stability, indicated the requirement of 6% CMS-2 emulsion to properly coat the selected aggregate. For the base material, it was established that the total fluids content (water, asphalt and moisture in the aggregates) must be controlled in the range of  $8\pm 0.5\%$  to enable adequate and convenient compaction. For the slurry seal, proper coating of the aggregate without runoff was generally obtained when the moisture content of the aggregate was approximately 2.0%.

Emulsion stabilization provides the mineral skeleton of the base with distinct mechanical properties. The residual bitumen on an emulsion-stabilized base selectively adheres to the smaller particles forming a binding mastic, which in turn binds the larger particles together. This mastic is very stiff under rapidly applied traffic loading but behaves like a membrane under the slow loading of subgrade movement. Under loading due to subgrade movement, the emulsion stabilized base material does not creep but the layer follows the underlying material's movement without cracking. When compacted under optimum fluid content, the granular matrix in the emulsion-stabilized base has similar internal friction as HMA. However, the surface of such a stabilized base is relatively fragile and prone to raveling. Therefore the surface has to be slurry sealed to attain strengths comparable to HMA.

### **Summary of Literature Review**

The literature search identified a variety of methods for the characterization of asphalt emulsions and emulsion residues. Among them are a number of disparate studies, including a

pre-SHRP effort, indicating the potential use of the current Superpave binder specifications to obtain emulsion residue physical properties that can be related to field performance. One of the most critical issues is finding the right method of residue recovery from the emulsions that would result in a sample representative of field conditions. The current high temperature distillation procedures have been found to adversely affect the microscopic structure of the residue, especially for polymer modified asphalt binders. A new method of forced airflow drying under ambient temperatures has been found to yield residues that adequately represent field conditions. For specification purposes, the emulsion can be dried in the RTFO at 85°C for 75 minutes without harming the microscopic structure of the residue.

A recent research effort sponsored by MnDOT showed that material evaluation is a critical aspect of CIR. The study indicated that RAP must be characterized in terms of moisture content, asphalt content and source gradation and that RAP gradations generally have very high variability. The total emulsion content is influenced by the asphalt content in the RAP and in turn influences the amount of air voids. Weather conditions during construction play an important role in the curing and performance of recycled pavements.

Based on the literature search the recovery methods proposed by Takamura were selected to obtain the residues used in the analysis. The current Superpave binder specifications were selected to determine the physical properties of the emulsion residues. The specifications included the newly proposed MP1a procedure. This allowed for a better comparison between the “conventional” asphalt binders and the asphalt emulsion residues and also allowed the prediction of the complex dynamic modulus of a typical CIR mixture based on the 2002 Design guide equations. Most of the research proposed in this study has not been done before based on the published information available to the authors at the time of this literature search.

# **CHAPTER 3**

## **RESEARCH METHODOLOGY**

### **Introduction**

This report summarizes the experimental work done at the University of Minnesota pavement materials laboratory as part of this project. A description of the materials used, as well as the testing hardware, is included. A description of the laboratory curing and testing of emulsions is presented.

### **Materials**

The goal of this project was to develop a method to determine asphalt emulsions properties that can be related to field performance with emphasis on emulsions used in cold in-place applications.

Four asphalt emulsions were chosen in this study. Three of them are commonly used in cold in-place recycling applications, CSS-1, EE (a proprietary engineered emulsion), and HFMS-2. The fourth one, CRS-2P, is used in seal coat applications and was included in the analysis for comparison purposes.

### **Equipment**

The asphalt emulsions were tested using standard Superpave binder test procedures. Long-term aging was simulated through a Prentex Pressure Aging Vessel (PAV) and degassing oven. Low temperature tests were performed with the Cannon Thermoelectric Bending Beam Rheometer (BBR) and Bohlin Direct Tension Tester (DT). High and intermediate temperature tests were performed using the Rheometrics RAA Dynamic Shear Rheometer (DSR).

### **Curing**

The asphalt residue was recovered from the emulsions using two different curing methods, following procedures outlined by Takamura [2]. The goal was to evaluate two different procedures to obtain the residue in terms of both practicality and testing results.

The first curing procedure involved simply air-drying the material. A 50g emulsion sample was placed in a PAV pan and allowed to stand for 24 hours at room temperature (~ 23°C). The sample was then placed in an oven at 60°C for 2 hours in order to remove any remaining moisture. The remaining residue was collected in tins for further testing.

The second curing procedure was a new rapid residue recovery procedure based on the Rolling Thin Film Oven Test (RTFOT). In this procedure, 35g of emulsion sample was poured in each bottle and placed in the carousel. The sample was dried at a temperature of 85°C for 75 minutes with a forced airflow of 4 L/min. The remaining residue was poured into one container and then distributed into smaller tins for further testing. One drawback to this procedure is that the emulsion residue adheres to the bottle, making it necessary to scrape every bottle in order to obtain reasonable amounts of residue for testing.

A portion of asphalt residue that was air-dried was further aged in the PAV. This was done in order to be able to apply the current asphalt binder specifications to the emulsion residues. It is not known if the PAV condition is truly representative of the aging process of the binder in CIR field mixtures. Pans were filled with 50g of residue and subjected to a temperature of 100°C and pressure of 2.10 MPa for 20 hours. Afterward, the sample was placed in a vacuum oven at 170°C and a pressure of 15 kPa absolute for 30 minutes in order to remove any air bubbles in the sample.

As a result, three conditions of asphalt emulsion residue were obtained: curing by air, curing by RTFOT, and curing by air followed by PAV (designated PAV hereafter). These materials were tested following the testing matrix shown in Table 3.1.

**Table 3.1. Testing Matrix**

Emulsion	DSR – Large Plate			DSR – Small Plate			BBR			DT		
	Air	RTFOT	PAV	Air	RTFOT	PAV	Air	RTFOT	PAV	Air	RTFOT	PAV
CRS-2P	X	X		X	X	X	X	X	X	X	X	X
CSS-1	X	X		X	X	X	X	X	X	X	X	X
EE	X	X		X	X	X	X	X	X	X	X	X
HFMS-2P	X	X		X	X	X	X	X	X	X	X	X

### Testing Procedures

For the conditions mentioned in Table 3.1, the following tests were conducted on the emulsion residue.



### *Bending Beam Rheometer*

Each emulsion was tested at two temperatures with two beams at each temperature. Testing procedures followed AASHTO TP1: Standard Test Method for Determining the Flexural Creep Stiffness of Asphalt Binder Using the Bending Beam Rheometer (BBR). Beams were placed in the controlled temperature bath for 1 hour prior to testing. The test measures the mid-point deflection of a simply supported asphalt beam subjected to a constant load of 980 mN for 240 seconds. The load and deflection were measured with time, and the bending stress was calculated from the dimensions of the beam, the span length, and the load. The bending strain was calculated from the dimensions of the beam and the deflection. Using the correspondence principle, the flexural creep stiffness was calculated with the following equation:

$$S(t) = \frac{PL^3}{4bh^3\delta(t)} \quad (3.1)$$

where:

$S(t)$  = time-dependent flexural creep stiffness, MPa

$P$  = constant load, N

$L$  = span length, mm

$b$  = beam width, mm

$h$  = beam thickness, mm

$\delta(t)$  = beam deflection, mm, as a function of time

The response of the test beam to the creep loading was plotted as  $\log(\text{stiffness})$  vs.  $\log(\text{time})$ . Over the testing time, the stiffness data can be represented by a second-order polynomial as follows:

$$\log S(t) = A[\log(t)]^2 + B[\log(t)] + C \quad (3.2)$$

and the slope,  $m$ , of the curve is equal to:

$$m(t) = \left| \frac{d[\log S(t)]}{d[\log(t)]} \right| = |2A[\log(t)] + B| \quad (3.3)$$

Using Excel, a trendline was fit to the stiffness data using the form in equation 3.2. The coefficients  $A$ ,  $B$ , and  $C$  were obtained and used to calculate the  $m$ -value using equation 3.3. The estimated values of the stiffness and  $m$  at 60 seconds are used for specification purposes.

### *Direct Tension*

Each emulsion was tested at two temperatures with six samples at each temperature. Testing procedures followed AASHTO TP3: Standard Test Method for Determining the Fracture Properties of Asphalt Binder in Direct Tension (DT). Samples were placed in the controlled temperature bath for 1 hour prior to testing. The test measures the stress and strain at failure in an asphalt binder test specimen pulled at a constant rate of elongation of 3% per minute. A displacement transducer is used to measure the elongation of the test specimen, and the load is monitored during the test. The tensile strain and stress at fracture are reported as the failure strain and stress, respectively.

### *Dynamic Shear Rheometer*

Extensive testing was done with the DSR for the purpose of constructing master curves. Testing procedures followed AASHTO TP5: Standard Test Method for Determining the Rheological Properties of Asphalt Binder Using a Dynamic Shear Rheometer (DSR). For the air and RTFOT cured specimens, tests were done on the small plate (8 mm) at intermediate temperatures and on the large plate (25 mm) at high temperatures. For the PAV aged material, tests were only performed on the small plate at intermediate temperatures. The test temperatures are shown in Table 3.2.

**Table 3.2. DSR Test Temperatures**

<b>Temperature, °C</b>	<b>Plate</b>
10	SP
16	SP
22	SP
28	SP
34	SP
40	LP, SP
46	LP
52	LP
58	LP
64	LP

In this test the absolute value of the complex shear modulus,  $|G^*|$ , and the phase angle,  $\delta$ , of the asphalt emulsion residue are determined. Test specimens were 1 mm thick for the large

plate and 2 mm thick for the small plate. Frequency sweeps were performed from 1 to 100 rad/s. The strain amplitude was adjusted in order to keep the torque amplitude between 2 and 50 g-cm. This ensured that the measurements were within the region of linear behavior and above the machine resolution limit. Strain values ranged from 0.2 to 200%, depending on the temperature and frequency tested. The test specimen was maintained at the test temperature in a forced air chamber. The complex modulus and phase angle were calculated automatically as part of the operation of the rheometer. Specification testing with the DSR is performed at a frequency of 10 rad/s.

#### *Additional Tests*

During the initial phase of laboratory testing it became apparent that, given the limited funding available, the project would benefit more from an expanded evaluation of the physical properties of the emulsions rather than performing a limited laboratory experiment to study the interaction between the asphalt emulsions and the RAP binder as a function of time and temperature. The additional experiments performed consisted of DSR frequency sweeps at different temperature to develop rheological master curves and critical cracking temperature,  $T_{crit}$ , determination from BBR and DT data according to AASHTO MP1a. These additional tests were selected based on the fact that at both the AASHTO and TRB Expert Task Group levels there is a sustained effort to introduce  $T_{crit}$  and master curve development as part of the future asphalt binder specifications.



# CHAPTER 4

## RESULTS AND DISCUSSION

### Introduction

The results obtained by performing the laboratory tests described in Chapter 3 were used to determine the PG grade for the four emulsion residues following the AASHTO MP1 procedure used for asphalt binders. Bending Beam Rheometer (BBR) and Direct Tension (DT) tests were performed to determine the low temperature limit, and the Dynamic Shear Rheometer (DSR) was used to calculate the high and intermediate limiting temperatures of the emulsion residues. Additional analysis was performed according to AASHTO MP1a to find the critical temperature for low-temperature cracking. Master curves were constructed from DSR stiffness data as an additional analysis tool.

### Performance Grade Analysis

#### *Dynamic Shear Rheometer*

Each emulsion residue was tested over a wide range of temperatures and frequencies for the purpose of constructing master curves. The AASHTO MP1 specification requires testing at only two temperatures and a single frequency of 10 rad/s. Because asphalt emulsions eliminate the need for hot mix plant operations, the residue was considered approximately equivalent to an RTFOT-aged binder, and therefore the limiting DSR criterion of 2.2 kPa for  $|G^*|/\sin\delta$  was selected. The test data at 10 rad/s was extracted from the data file and is presented in Table 4.1. The high temperature limits were determined from DSR data obtained at two temperatures and 10 rad/s, assuming that that  $\log(|G^*|/\sin\delta)$  varied linearly between the two selected temperatures.

The results in Table 4.1 indicate that for the four emulsions tested, the curing technique affected the high limiting temperatures. The RTFOT cured specimens had higher limiting temperatures than the air-cured specimens, with differences ranging between 0.7°C for EE to 3.4°C for CRS-2P, indicating that the RTFOT curing procedure resulted in stiffer residues. It is not clear if this difference was due to a higher rate of oxidation occurring in the RTFOT procedure or to the fact that small amounts of water was still present in the air-cured specimens.

Similar calculations were performed for the PAV aged samples to determine the temperature at which  $|G^*|\sin\delta$  is 5000 kPa. The results of the DSR tests on PAV material are shown in Table 4.2. The limiting temperatures were determined by assuming a linear relationship between  $\log(|G^*|\sin\delta)$  and the test temperature.

**Table 4.1. DSR Results @ 10 rad/s, High Temperature**

	Emulsion	T, °C	$ G^* $ , Pa	$\delta$ , degree	$ G^* \sin\delta$ , kPa	T, °C, where $ G^* \sin\delta = 2.2$ kPa
Air	CRS-2P	58	2099.9	71.0	2.22	58.1
		64	1138.6	72.9	1.19	
	CSS-1	52	2879.8	84.6	2.89	54.0
		58	1259.9	86.3	1.26	
	EE	46	2282.1	85.4	2.29	46.3
		52	951.6	87.0	0.95	
	HFMS-2P	52	2189.0	68.1	2.36	52.7
		58	1188.9	70.0	1.26	
RTFOT	CRS-2P	58	2933.1	69.0	3.14	61.5
		64	1605.5	70.9	1.70	
	CSS-1	52	3359.0	83.6	3.38	55.2
		58	1489.5	85.1	1.49	
	EE	46	2562.2	84.9	2.57	47.0
		52	980.8	86.7	0.98	
	HFMS-2P	52	2516.4	71.5	2.65	53.7
		58	1307.1	73.9	1.36	

**Table 4.2. DSR Results @ 10 rad/s, Intermediate Temperature**

	Emulsion	T, °C	$ G^* $ , kPa	$\delta$ , degree	$ G^* \sin\delta$ , kPa	T, °C, where $ G^* \sin\delta=5000$ kPa
PAV	CRS-2P	16	1900	52.8	1513	7.6
		22	768	56.8	642	
	CSS-1	16	4319	50.7	3341	13.2
		22	1706	56.7	1425	
	EE	16	1258	59.7	1086	6.5
		22	458	64.4	413	
	HFMS-2P	16	1750	54.5	1425	7.9
		22	651	59.3	560	

### *Bending Beam Rheometer*

Each emulsion residue was tested at two temperatures with the BBR. AASHTO MP1 requires the stiffness at 60 seconds to be less than 300 MPa and the  $m$ -value to be greater than 0.300. The test temperatures were selected to bracket these two requirements. Two samples were tested at each temperature and the results averaged. Repeatability of the test results was within the limits recommended by AASHTO. The creep stiffness ( $S$ ) was calculated at each step using equation 3.1. A plot was made of  $\log(S)$  vs.  $\log(\text{time})$ , and a second order polynomial was fit to the data using equation 3.2. The  $m$ -value was determined using equation 3.3. Table 4.3 shows a summary of the Bending Beam Rheometer test results. Stiffness limiting temperatures were obtained by linear interpolation assuming that  $\log(S)$  varies linearly with temperature. The  $m$ -value limiting temperature was determined assuming that  $m$ -value varied linearly with temperature.

Table 4.3 indicates that, similar to DSR testing, the curing method affects the limiting temperatures. The RTFOT cured specimens had higher limiting temperatures than the air-cured specimens, with the exception of EE residue, for both the  $S$  and the  $m$  limiting temperatures. These results confirm in part that RTFOT-cured samples may experience a higher rate of oxidation than the air-cured samples. As expected the limiting temperatures, for both the  $S$  and the  $m$  criteria, for the PAV-aged samples were higher than the air and RTFOT samples, indicating a stiffening effect combined with an increase in the relaxation time, as seen in conventional asphalt binders. For all three conditions the stiffness was the control criterion.

### *PG Grading*

Based on the test results previously described and the MP1 criteria for RTFOT and PAV conditions “PG” grades were determined for the emulsion residues investigated. The grades are summarized in Table 4.4. As expected the CRS-2P emulsion that is used in surface treatments applications had the largest high-temperature limit. Note that the two curing conditions, the RTFOT-cured and the air-cured, did not change the grades of the residues. It should also be noted that emulsions in general are climate-designed and the “performance-grades” determined in this study are typical for emulsion applications used in Minnesota type of climate; a CSS-1 used in a different location may have a different “performance-grade.”

**Table 4.3. Bending Beam Rheometer Results**

	Emulsion	T, °C	S(60s), MPa	m(60s)	T, °C, where S(60s)=300 MPa	T, °C, where m(60s)=0.300
<b>Air</b>	CRS-2P	-24	141.9	0.394	<b>-28.9</b>	<b>-30.0</b>
		-30	354.3	0.300		
	CSS-1	-24	283.9	0.357	<b>-24.4</b>	<b>-26.9</b>
		-30	602.6	0.241		
EE	-24	134.0	0.448	<b>-28.5</b>	<b>-32.1</b>	
	-30	389.5	0.339			
HFMS-2P	-30	162.8	0.383	<b>-35.1</b>	<b>-35.7</b>	
	-36	332.0	0.296			
<b>RTFOT</b>	CRS-2P	-24	176.7	0.383	<b>-27.5</b>	<b>-29.6</b>
		-30	433.1	0.294		
	CSS-1	-24	243.9	0.358	<b>-25.5</b>	<b>-27.2</b>
		-30	558.8	0.249		
EE	-24	145.1	0.452	<b>-28.3</b>	<b>-31.5</b>	
	-30	397.4	0.331			
HFMS-2P	-30	203.7	0.373	<b>-32.8</b>	<b>-34.7</b>	
	-36	463.7	0.280			
<b>PAV</b>	CRS-2P	-24	221.1	0.347	<b>-26.2</b>	<b>-27.5</b>
		-30	499.6	0.266		
	CSS-1	-18	150.8	0.379	<b>-22.4</b>	<b>-23.5</b>
		-24	384.3	0.293		
EE	-24	191.3	0.383	<b>-27.4</b>	<b>-29.4</b>	
	-30	426.0	0.292			
HFMS-2P	-24	167.0	0.361	<b>-28.8</b>	<b>-29.5</b>	
	-30	349.6	0.294			

**Table 4.4. Asphalt Emulsion Residue “Performance Grades”**

Emulsion	Performance Grade
CRS-2P	58-34
CSS-1	52-28
EE	46-34
HFMS-2P	52-34

*Direct Tension*

Each asphalt emulsion was tested at two temperatures in the Direct Tension Tester, with six specimens at each temperature. Tests were performed on PAV aged material at the same temperatures as the BBR. This test is optional in AASHTO MP1, but it can be used in lieu of the



creep stiffness requirement from the BBR, as long as the  $m$ -value requirement is met. Samples were prepared and placed in a constant temperature bath for one hour prior to testing. They were pulled in tension at a constant rate of 3% per minute, and the stress and strain at failure were determined. Test results are shown in Table 4.5. For two of the residues the failure strain crossed 1%, while for the other two the strains were below 1% at both test temperatures. The failure strain limiting temperature was calculated by assuming a linear relation between  $\log(\epsilon_f)$  and test temperature. Coefficients of variation (CV) were calculated for both the failure stress and failure strain data.

**Table 4.5. Direct Tension Test Results**

	Emulsion	T, °C	Failure Stress, MPa	Failure Strain, %	CV ( $\sigma$ ), %	CV ( $\epsilon_f$ ), %	T, °C, where $\epsilon_f = 1\%$
Air	CRS-2P	-18	0.77	5.03	3.3%	0.1%	<b>-29.8</b>
		-24	1.40	2.22	9.1%	13.7%	
	CSS-1	-18	1.06	2.45	13.9%	33.2%	<b>-21.6</b>
		-24	1.07	0.55	19.8%	22.3%	
	EE	-24	0.95	1.50	17.0%	22.3%	<b>-25.6</b>
		-30	0.60	0.32	23.6%	29.6%	
	HFMS-2P	-30	1.16	2.38	34.3%	54.9%	<b>NA</b>
		-36	NA	NA	NA	NA	
RTFOT	CRS-2P	-24	1.53	1.73	9.4%	21.9%	<b>-30.8</b>
		-30	1.66	1.07	33.7%	12.0%	
	CSS-1	-18	0.78	1.51	20.0%	37.8%	<b>-20.3</b>
		-30	0.62	0.18	27.1%	27.7%	
	EE	-24	0.70	1.30	24.9%	18.6%	<b>-25.5</b>
		-30	0.73	0.45	46.1%	22.0%	
	HFMS-2P	-30	0.83	1.27	32.0%	54.3%	<b>NA</b>
		-36	NA	NA	NA	NA	
PAV	CRS-2P	-24	1.54	1.36	12.7%	21.5%	<b>-25.3</b>
		-30	0.99	0.32	13.9%	17.1%	
	CSS-1	-18	0.78	0.81	39.8%	57.0%	<b>-16.1</b>
		-24	1.04	0.42	30.0%	38.0%	
	EE	-24	0.61	0.52	48.0%	42.5%	<b>-15.9</b>
		-30	0.83	0.32	22.0%	19.8%	
	HFMS-2P	-24	1.09	1.31	11.1%	17.8%	<b>-25.2</b>
		-30	0.74	0.33	22.6%	26.4%	

A number of observations can be made from Table 4.5. The curing method seems to play a much smaller role with respect to the limiting temperature as compared to DSR and BBR test

data. As expected, the PAV limiting temperatures are much higher than the unaged samples indicating significant aging (or other chemical modification) especially in the EE residue for which the limiting temperature increased by almost 10°C. One very important observation is the relatively small strength values measured in all four residues; the highest value is 1.54 MPa with most of the values being under 1 MPa. For some of the conventional polymer-modified binders the strength values can be as high as 7 MPa.

## **AASHTO MP1a Analysis**

### *Thermal Stress Calculations*

The analysis method presented in this section is described in detail by Basu [12]. AASHTO MP1a specifications require thermal stress calculations based on stiffness master curves obtained from BBR data. The master curves are generated by fitting the Christensen-Anderson-Marasteanu (CAM) model to the BBR stiffness data obtained at two temperatures:

$$S(t) = S_{glassy} \left[ 1 + \left( \frac{t}{t_c} \right)^v \right]^{-\frac{w}{v}} \quad (4.1)$$

where

$S(t)$  = Stiffness at a reduced time  $t$  (MPa)

$S_{glassy}$  = 3 GPa, assumed constant

$t_c$ ,  $w$ ,  $v$  = parameters in the model

The calculations are based on the assumptions that time-temperature superposition holds and that the effects of physical hardening can be neglected. This approach incorporates a thermo-viscoelastic model to describe the residue behavior at cold temperatures and requires both BBR and DT test data. The model uses an empirical parameter, the Pavement Constant (PC), to convert binder thermal stresses to mixture thermal stresses. This concept should be used with caution, as there is no field data to verify the existence of a Pavement Constant for CIR applications. In general, the concept of a constant value regardless of pavement structure and mixture type is debatable among researchers.

The thermal stress calculations were performed with software developed at the University of Minnesota. The software converts the creep compliance to relaxation modulus, fits the CAM model to the relaxation modulus and solves the hereditary integral. The program uses a 24-point

Gaussian integration to numerically integrate the convolution integral to calculate the binder thermal stresses at each 0.5°C interval from 22°C to -40°C. The binder thermal stress is then multiplied by a Pavement Constant to obtain the mixture thermal stress. Two different values of PC were used for comparison, PC = 24 and PC = 18 (recommended in MP1a). The thermal stress development with temperature and the strength data from the Direct Tension test are plotted together and the intersection of the two curves determines the critical cracking temperature,  $T_{cr}$ . Thermal stress and strength curves for the PAV-aged emulsions are shown in Figures 4.1 through 4.4.

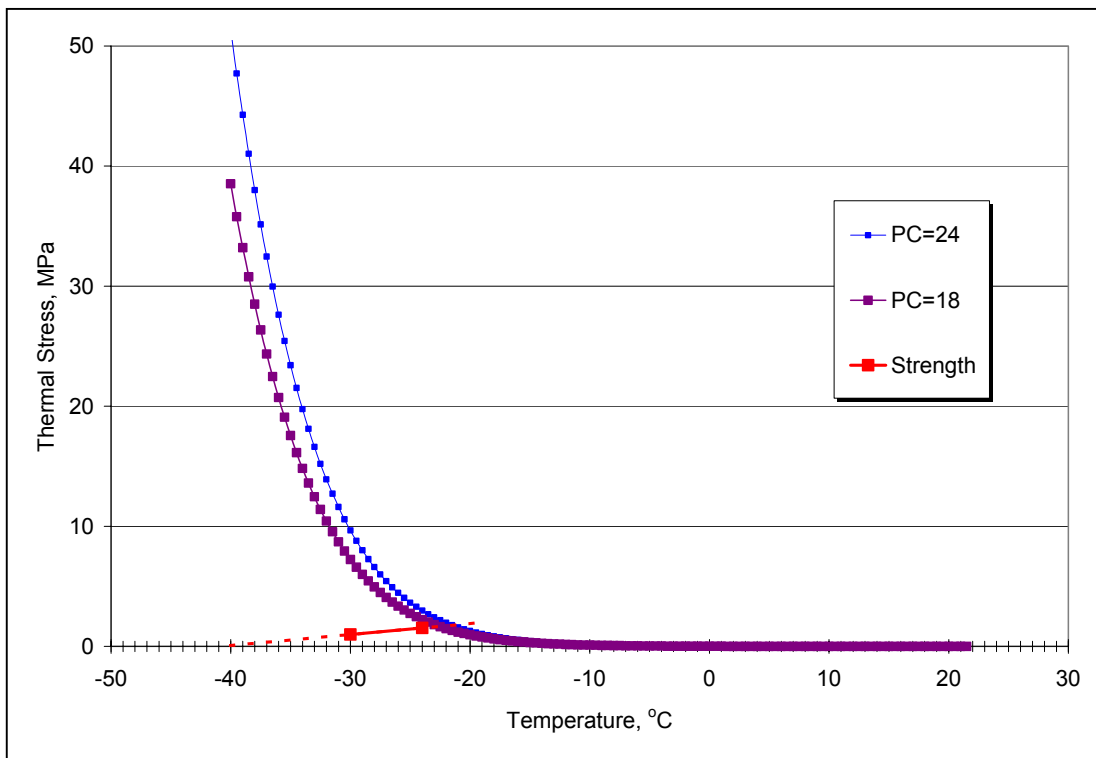


**Figure 4.1. Thermal Stress, Strength vs. Temperature (CRS-2P PAV)**

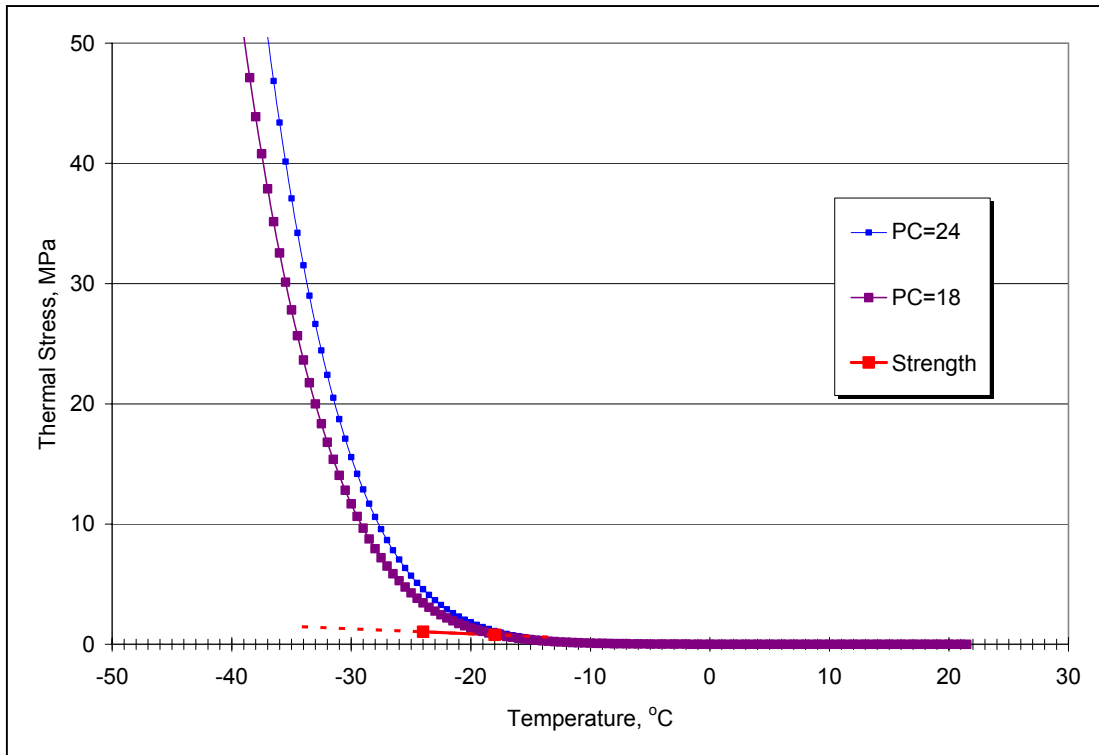


**Figure 4.2. Thermal Stress, Strength vs. Temperature (CSS-1 PAV)**

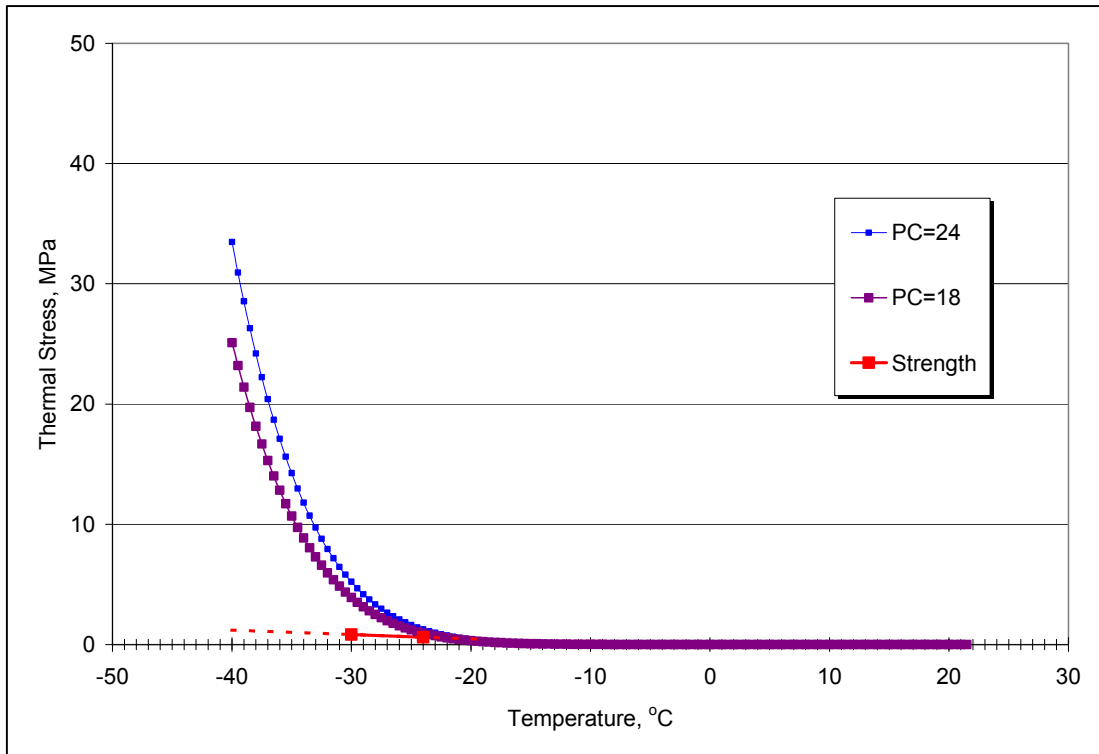


**Figure 4.3. Thermal Stress, Strength vs. Temperature (EE PAV)**

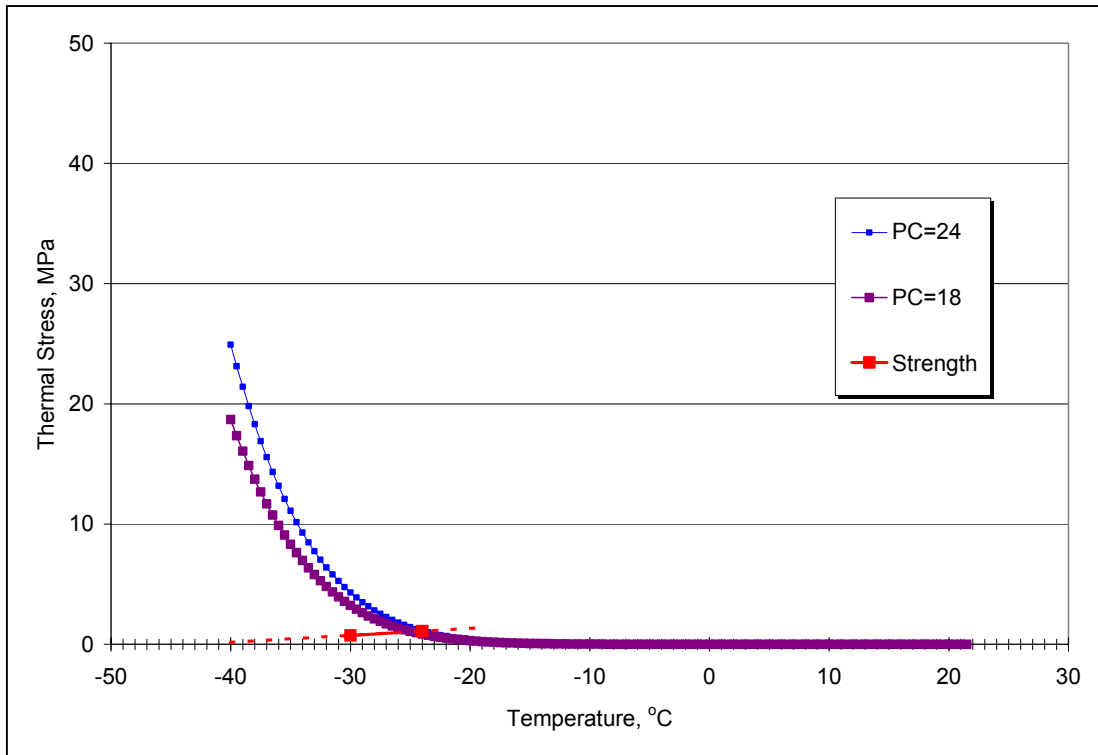


**Figure 4.4. Thermal Stress, Strength vs. Temperature (HFMS-2P PAV)**

A comparison of the limiting temperatures obtained from MP1 and  $T_{cr}$  from MP1a is shown in Table 4.6. Note that the PG limiting temperatures were calculated by subtracting 10°C from the temperature values obtained by linear interpolation of the test data. No subtraction is necessary for the MP1a critical temperature.

**Table 4.6. Critical Cracking Temperature**

		PG Limiting Temperatures, °C			MP1a $T_{cr}$ , °C	
	Emulsion	S(60s) = 300MPa	m(60s) = 0.300	$\epsilon_f = 1\%$	PC = 24	PC = 18
<b>Air</b>	CRS-2P	-38.9	-40.0	-39.8	-25.9	-27.3
	CSS-1	-34.4	-36.9	-31.6	-20.6	-21.7
	EE	-38.5	-42.1	-35.6	-25.5	-26.2
	HFMS-2P	-45.1	-45.7	NA	-29.8	-31.2
<b>RTFOT</b>	CRS-2P	-37.5	-39.6	-40.8	-24.7	-25.9
	CSS-1	-35.5	-37.2	-30.3	-21.9	-22.8
	EE	-38.3	-41.5	-35.5	-25.0	-25.9
	HFMS-2P	-42.8	-44.7	NA	-29.0	-29.9
<b>PAV</b>	CRS-2P	-36.2	-37.5	-35.3	-21.6	-22.7
	CSS-1	-32.4	-33.5	-26.1	-16.3	-17.7
	EE	-37.4	-39.4	-25.9	-20.2	-21.7
	HFMS-2P	-38.8	-39.5	-35.2	-23.9	-24.8

A number of observations can be made from Table 4.6. The limiting temperatures from the S and *m* criteria are within 2°C of each other. However, the failure strain limiting temperature differs from the BBR limiting temperatures by values as high as 11.5°C for EE PAV-aged residue. The PAV aging seems to have a much stronger effect on the fracture properties of the emulsion residues than on the stiffness properties. The most significant difference however is observed between the PG limiting temperatures and the MP1a critical temperature values. For conventional asphalt binders these values are in general reasonably similar and do not significantly affect the grade of the material. For the four residues the differences are very significant with most of the  $T_{cr}$  values being at least 10°C higher than the PG limiting values. This is due to the low strength values measured for all four residues as compared to regular binders. It is not clear why the strength is so small in the residue samples investigated.

### DSR Master Curves

Dynamic Shear Rheometer (DSR) data was used to construct master curves for each of the residues. Tests were performed at 6°C temperature increments from 10 to 64°C using frequency sweeps from 1 to 100 radians/second. The master curves were constructed by fitting the Christensen-Anderson-Marasteanu (CAM) model to the  $|G^*|$  data obtained with the DSR. The CAM model is as follows:

$$|G^*(\omega)| = G_g \left[ 1 + \left( \frac{\omega_c}{\omega} \right)^v \right]^{-\frac{w}{v}} \quad (4.2)$$

where

- $|G^*(\omega)| =$  absolute value of complex modulus as a function of frequency  $\omega$  (GPa)
- $G_g =$  glassy modulus ( $\log [G_g]$  is considered fixed at 9.1)
- $\omega_c, v, w =$  parameters in the model

The nonlinear regression routine in the commercial statistical software SigmaStat was used to fit the master curves for each emulsion residue at a reference temperature of 22°C. The shift factors for each temperature were determined as unknown parameters in the regression along with  $\omega_c$ ,  $v$ , and  $w$ . The regression parameters are summarized in Tables 4.7 to 4.9. Note that  $q = \log \omega_c$ .

**Table 4.7. CAM Model Parameters (Air)**

	<b>CRS-2P air</b>	<b>CSS-1 air</b>	<b>EE air</b>	<b>HFMS-2P air</b>
<b>q</b>	5.3748	3.2611	4.0301	6.1876
<b>v</b>	0.2248	0.1718	0.1654	0.2492
<b>w</b>	0.797	1.0712	1.0419	0.7625
<b>α10</b>	1.3385	1.3417	1.3508	1.2305
<b>α16</b>	0.6884	0.6718	0.6859	0.5753
<b>α22</b>	0	0	0	0
<b>α28</b>	-0.6717	-0.7507	-0.7996	-0.5969
<b>α34</b>	-1.181	-1.2837	-1.4221	-1.0783
<b>α40</b>	-1.5584	-1.7842	-1.6848	-1.5525
<b>α46</b>	-1.9936	-2.2295	-2.1367	-1.9427
<b>α52</b>	-2.4493	-2.6672	-2.5483	-2.3334
<b>α58</b>	-2.8248	-3.0482	-2.8885	-2.6824
<b>α64</b>	-3.1628	-3.3799	-3.1956	-2.9919

**Table 4.8. CAM Model Parameters (RTFOT)**

	<b>CRS-2P RTFOT</b>	<b>CSS-1 RTFOT</b>	<b>EE RTFOT</b>	<b>HFMS-2P RTFOT</b>
<b>q</b>	5.159	3.3665	4.1497	5.0831
<b>v</b>	0.2119	0.1751	0.1786	0.1736
<b>w</b>	0.787	1.0526	1.0492	0.8377
<b>α10</b>	1.3085	1.3326	1.2698	1.22
<b>α16</b>	0.6589	0.6597	0.6354	0.6089
<b>α22</b>	0	0	0	0
<b>α28</b>	-0.6915	-0.7422	-0.6677	-0.6787
<b>α34</b>	-1.2035	-1.2651	-1.1797	-1.2344
<b>α40</b>	-1.7015	-1.6948	-1.5573	-1.6811
<b>α46</b>	-2.1277	-2.1525	-1.997	-2.0873
<b>α52</b>	-2.5615	-2.6125	-2.4371	-2.5378
<b>α58</b>	-2.9328	-2.9903	-2.7786	-2.8968
<b>α64</b>	-3.2753	-3.3279	-3.0839	-3.2176

**Table 4.9. CAM Model Parameters (PAV)**

	<b>CRS-2P PAV</b>	<b>CSS-1 PAV</b>	<b>EE PAV</b>	<b>HFMS-2P PAV</b>
<b>q</b>	4.7451	2.2675	4.0805	4.6788
<b>v</b>	0.1793	0.1458	0.173	0.1803
<b>w</b>	0.7621	1.0353	0.9221	0.7907
<b>α16</b>	0.641	0.6742	0.6321	0.674
<b>α22</b>	0	0	0	0
<b>α28</b>	-0.6185	-0.714	-0.6981	-0.671
<b>α34</b>	-1.2138	-1.304	-1.339	-1.2335
<b>α40</b>	-1.7331	-1.8507	-1.8075	-1.7054

The  $|G^*|$  master curves for air-cured, RTFOT-cured and PAV-aged residues for each of the four residues are shown in Figures 4.5 to 4.8. With the exception of the data at 34°C for EE air, the data could be shifted to form smooth master curves. It is not clear why for the 34°C frequency sweep  $|G^*|$  started to decrease at the higher frequency end. The test was repeated twice with similar results.

These plots show that the PAV residue was stiffer than both air and RTFOT cured residue for all four emulsions, as expected. The air and RTFOT residues gave similar modulus values for the CSS-1 and EE emulsions, while the CRS-2P and HFMS-2P emulsions showed slightly higher modulus values for the RTFOT residues. The limited experimental data suggests that the air curing method results in more conservative rheological properties of the emulsion residues.

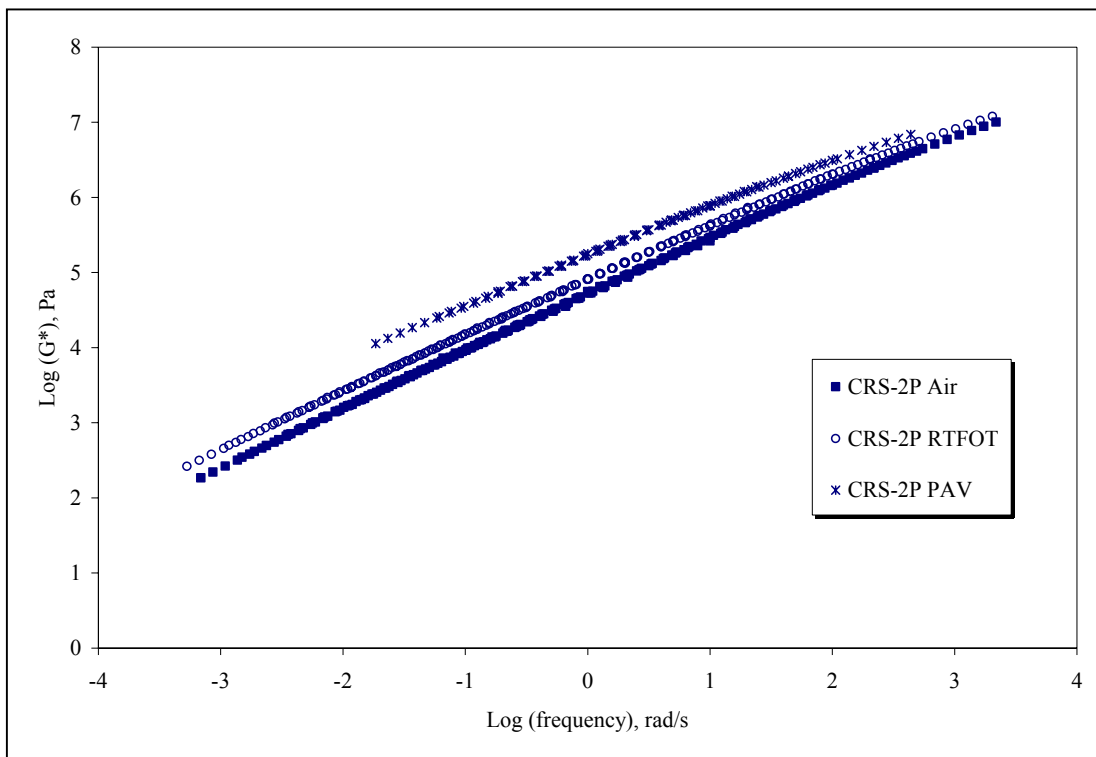


**Figure 4.5. DSR Stiffness Master Curve, CRS-2P**



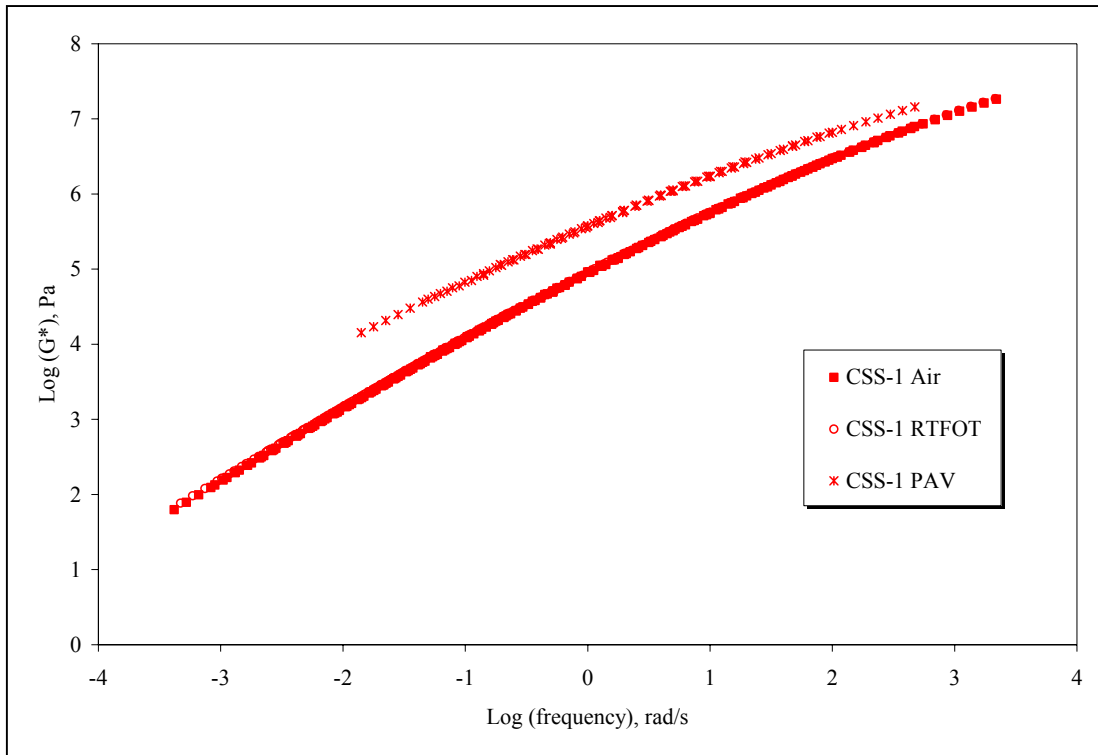


**Figure 4.6. DSR Stiffness Master Curve, CSS-1**

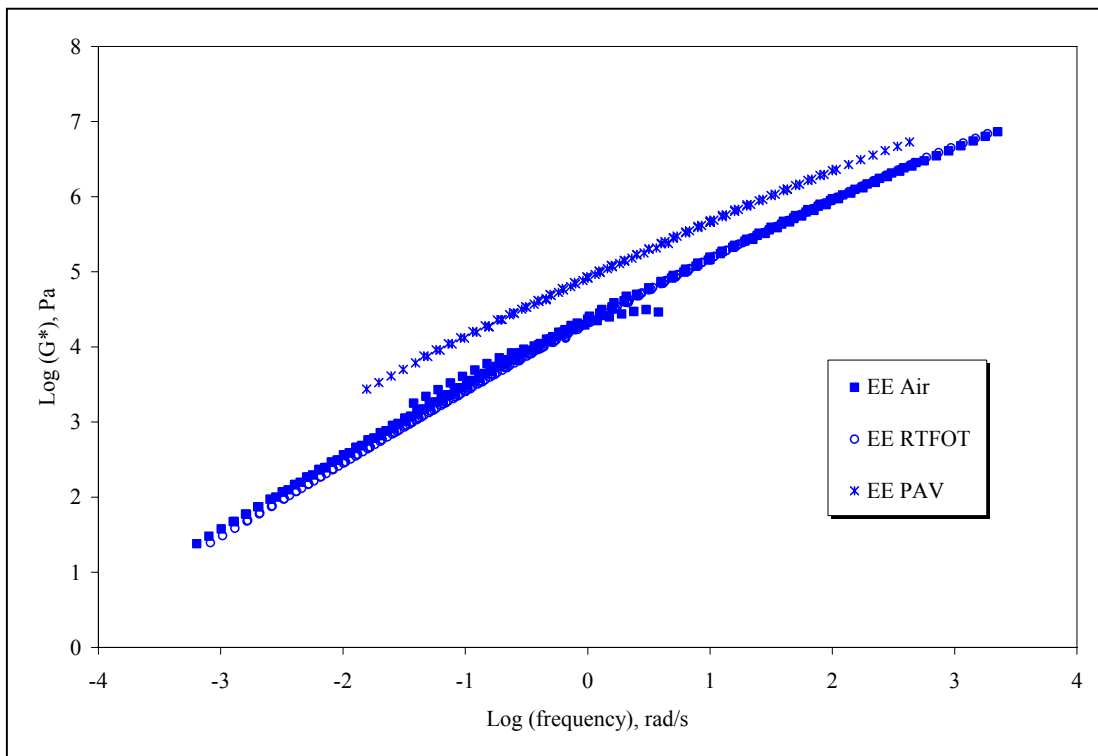


**Figure 4.7. DSR Stiffness Master Curve, EE**

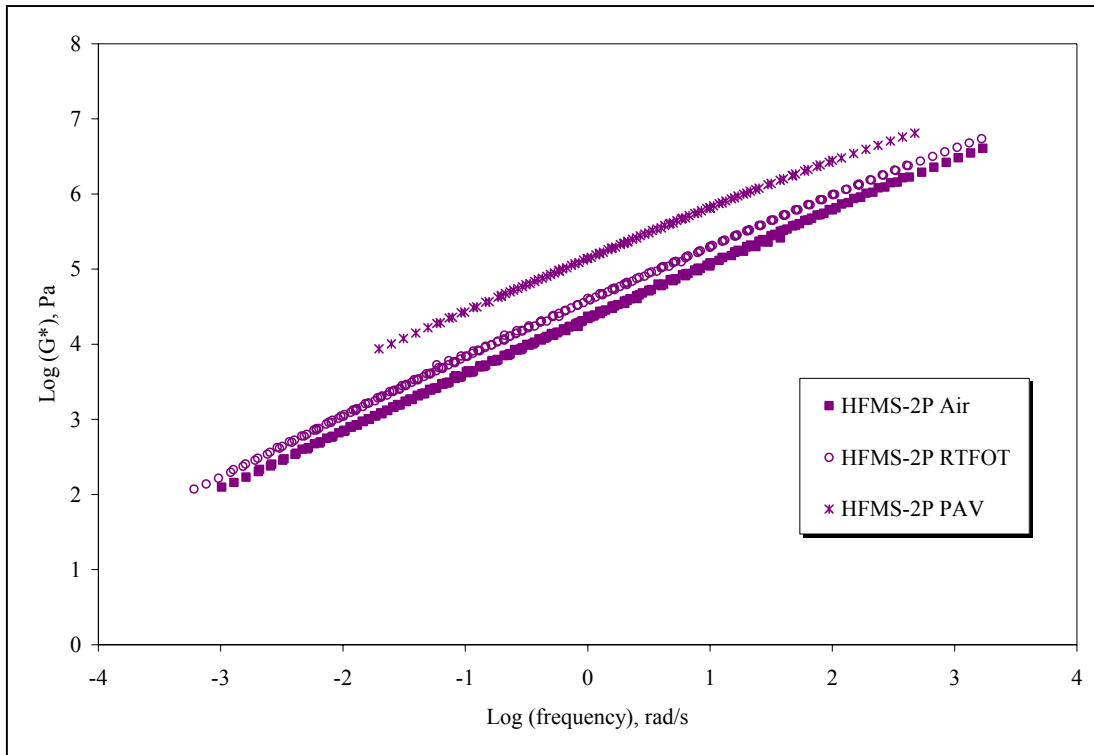


**Figure 4.8. DSR Stiffness Master Curve, HFMS-2P**

Figures 4.9 to 4.11 show the  $|G^*|$  master curves for each of the air-cured, RTFOT-cured, and PAV-aged conditions. The air and RTFOT residues showed similar behavior in Figures 4.9 and 4.10. At high frequencies, CSS-1 was stiffer than CRS-2P. However, the curves cross and at lower frequencies, CSS-1 became softer than CRS-2P. The larger slope for CSS-1 indicates that that emulsion is more susceptible to changes in temperature than CRS-2P. EE and HFMS-2P have similar stiffness values at high frequencies, but they begin deviating at lower frequencies so that EE becomes softer than HFMS-2P. Figure 4.11 shows that the PAV residue is much stiffer than the air and RTFOT residues, as expected. In addition, the curves seem to flatten out, which indicates that the stiffness does not change as much with temperature with respect to unaged residues. The PAV aging brings together the CRS-2P and HFMS-2P curves so that they show similar stiffness values with frequency.

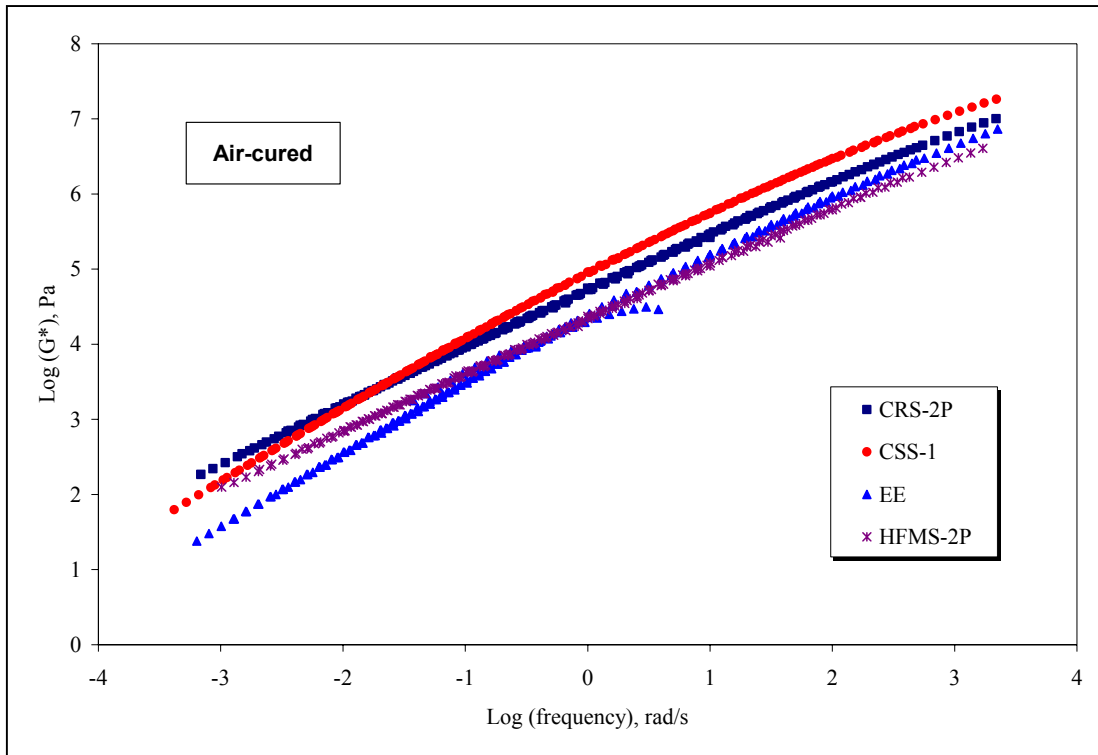


Figure 4.9. DSR Stiffness Master Curve, Air cured residue

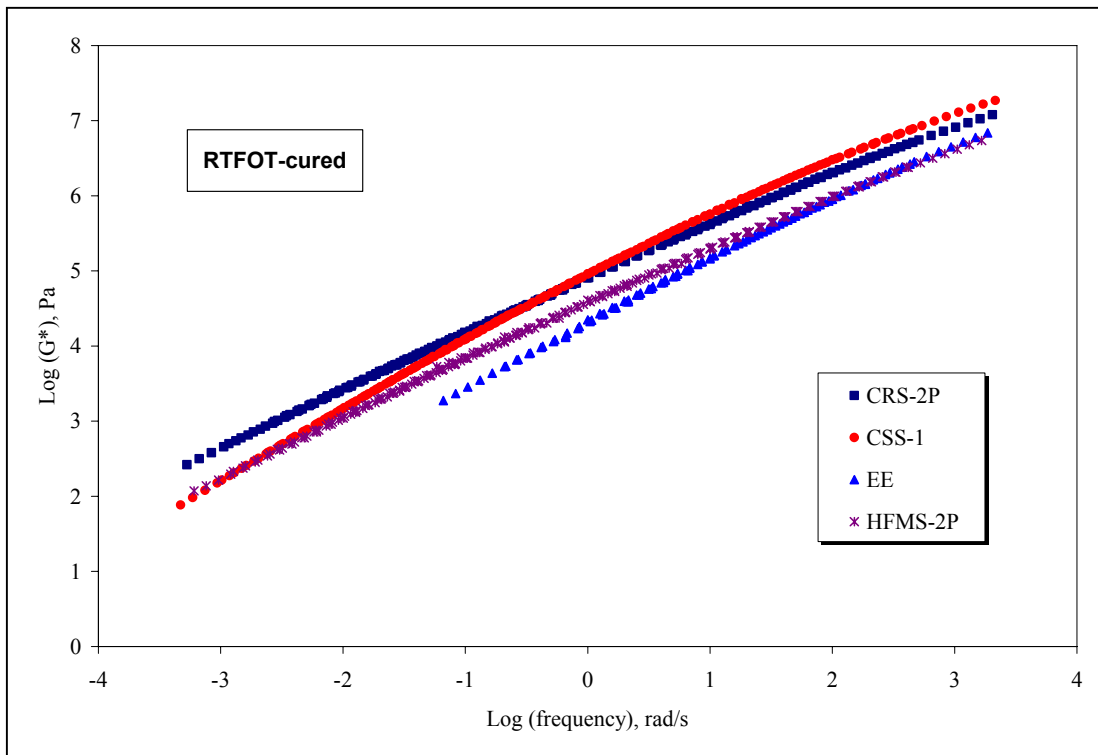
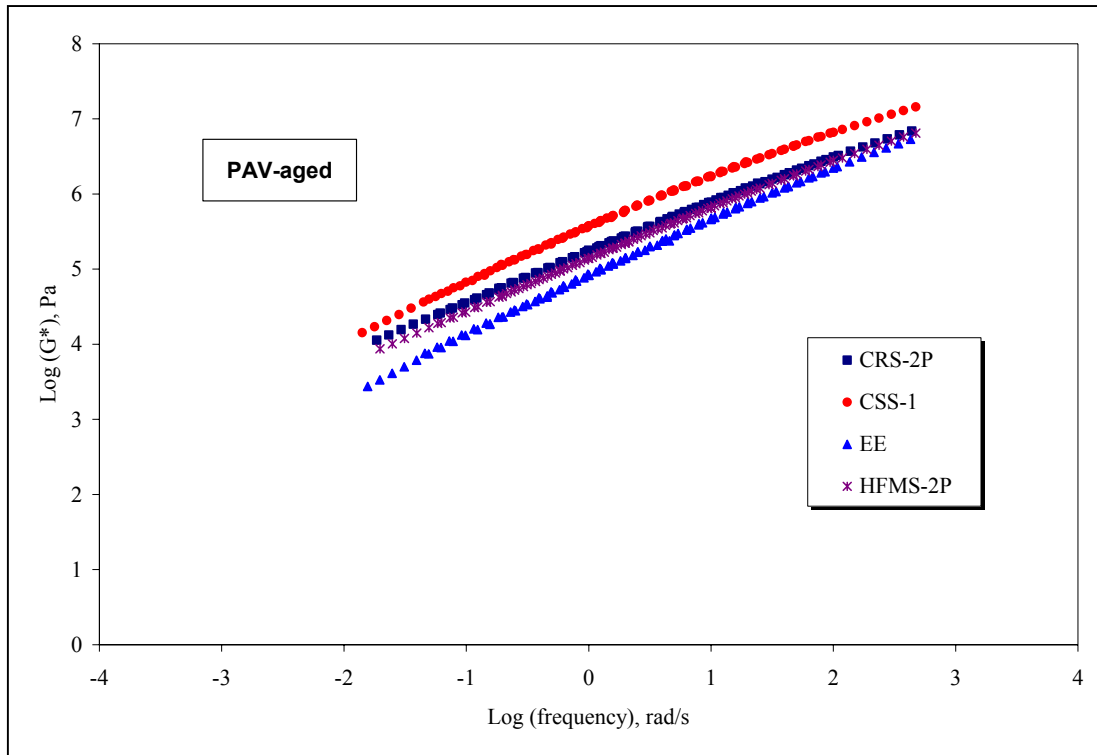


Figure 4.10. DSR Stiffness Master Curve, RTFOT cured residue



**Figure 4.11. DSR Stiffness Master Curve, PAV aged residue**

#### *Phase Angle Master Curves*

Master curves were also constructed of phase angle vs.  $\log(\omega)$ . The same shift factors that were used with the shear modulus were used to shift the phase angle data horizontally. Figures 4.12 to 4.15 show the phase angle master curves for CRS-2P, CSS-1, EE, and HFMS-2P, respectively. The curves for air-cured, RTFOT-cured, and PAV-aged residues are included on the plots.

The phase angle master curves are not very smooth indicating most probably the presence of small phase transitions or thixotropy effects, especially in the polymer modified samples. CRS-2P and HFMS-2P also show a pronounced plateau in phase angle, which is similar to the trend observed in conventional polymer-modified binders. CSS-1 and EE show similar phase angles for the air and RTFOT cured material. CRS-2P has a higher phase angle for the air-cured residue than the RTFOT residue throughout the entire range of frequencies. HFMS-2P has a higher phase angle at high frequencies for air than for RTFOT residue, but the trend reverses at low frequencies. In all cases, the phase angle for PAV residue is lower than air and RTFOT residues. This indicates a stiffer and more elastic material, which is expected.

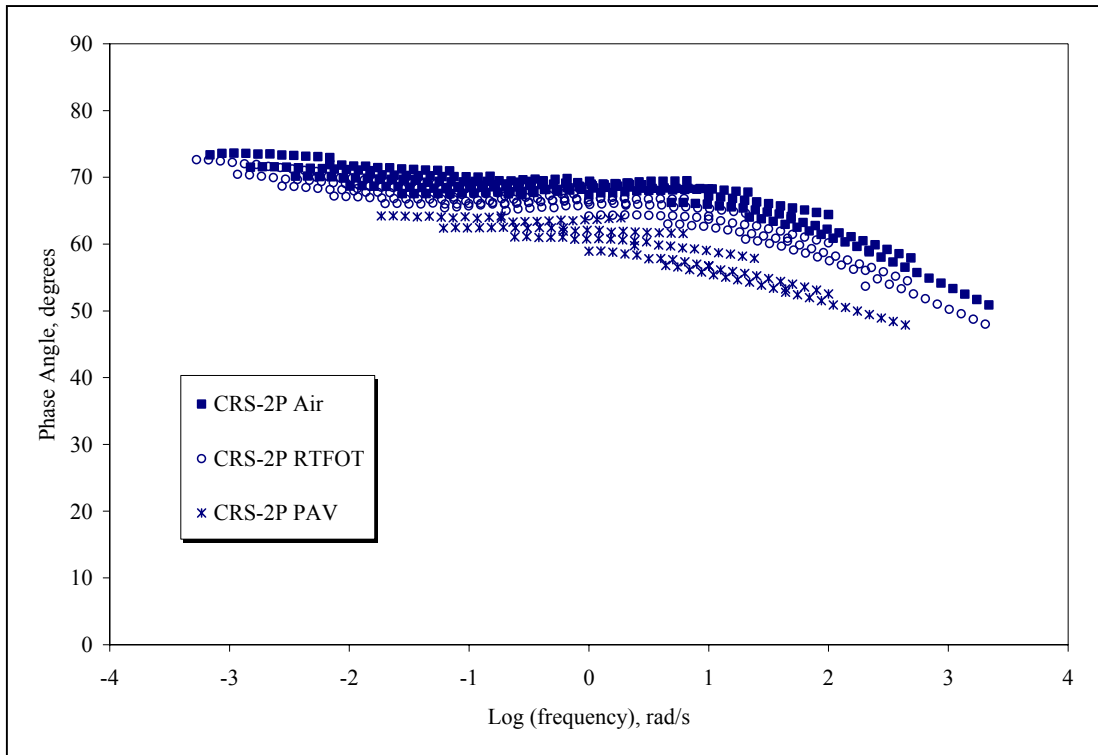


**Figure 4.12. DSR Phase Angle Master Curve, CRS-2P**

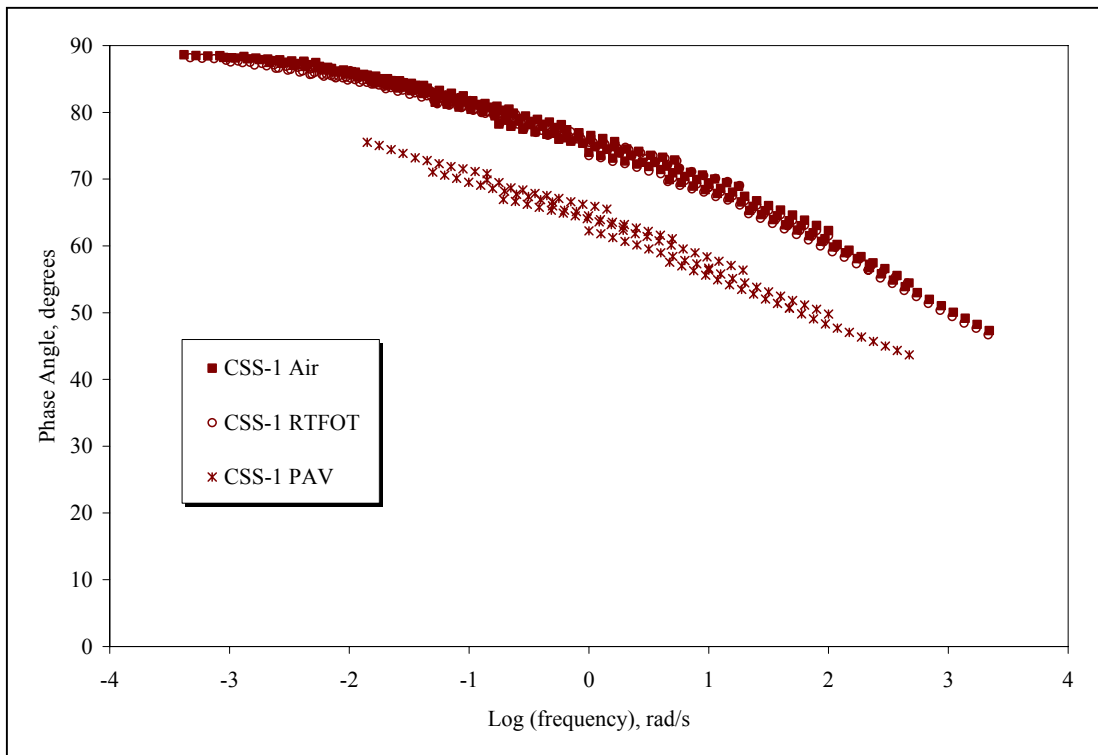


**Figure 4.13. DSR Phase Angle Master Curve, CSS-1**

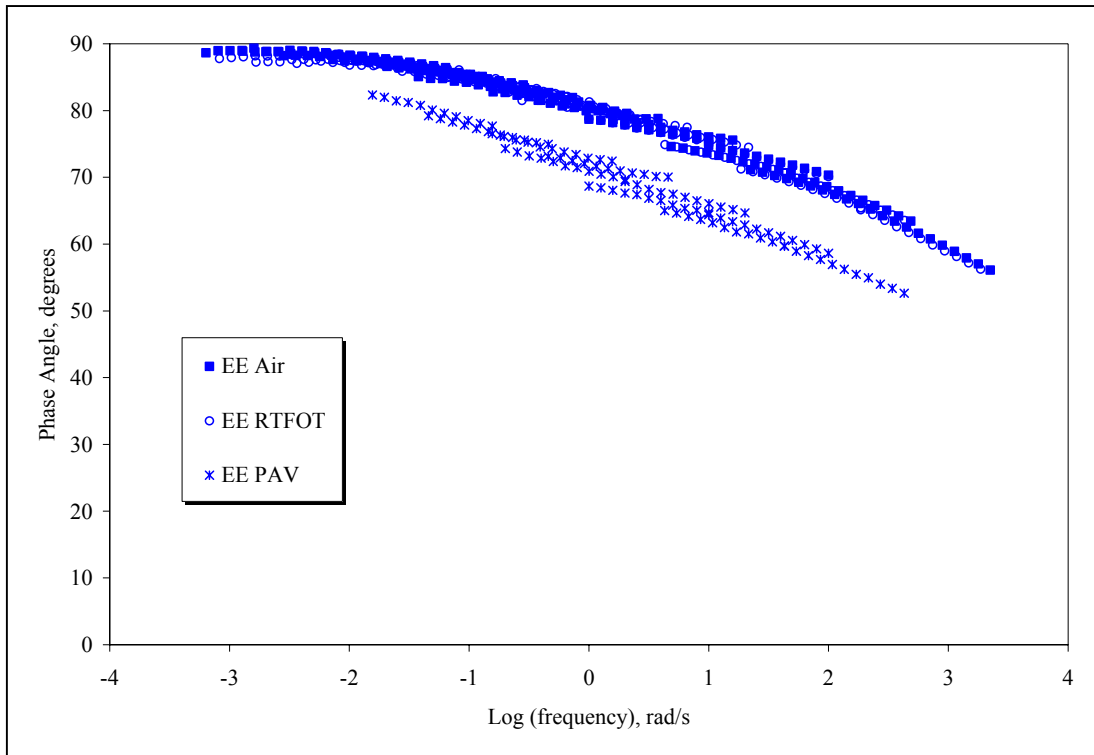


**Figure 4.14. DSR Phase Angle Master Curve, EE**

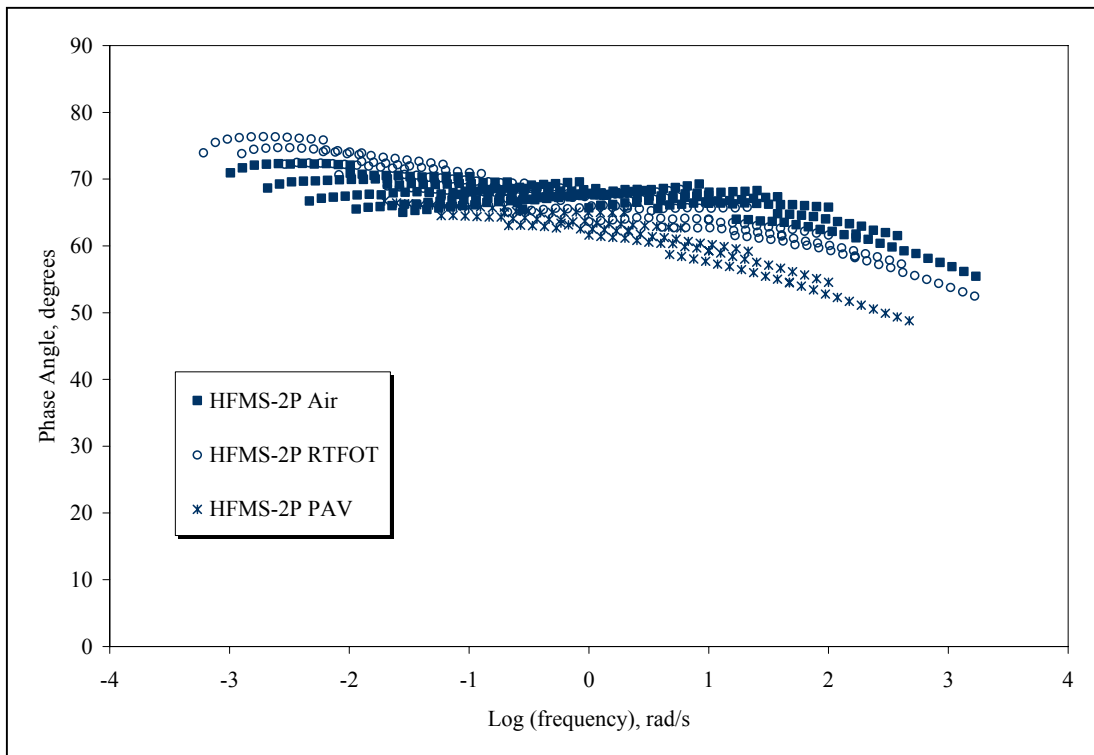


**Figure 4.15. DSR Phase Angle Master Curve, HFMS-2P**

Figures 4.16 to 4.18 show the phase angle master curves for air-cured, RTFOT-cured, and PAV-aged residues, respectively. Each of the four emulsions studied are included on the plots. CSS-1 and EE show the typical shape of expected master curves, although they are not completely smooth. There is a general downward trend of the phase angle with increasing frequency for these emulsions. CRS-2P and HFMS-2P, as already mentioned, are relatively flat and the phase angle does not change significantly with frequency. EE has the highest phase angle for all frequencies, followed by CSS-1. At high frequencies the phase angles for CRS-2P and HFMS-2P cross that of CSS-1. For the air-cured residues, CRS-2P and HFMS-2P have basically the same phase angle for the entire range of frequencies. For the RTFOT-cured residues, however, the phase angle for HFMS-2P was higher than that of CRS-2P. As expected, the phase angle for all four emulsions drops for the PAV material, indicating a stiffer or more elastic material.

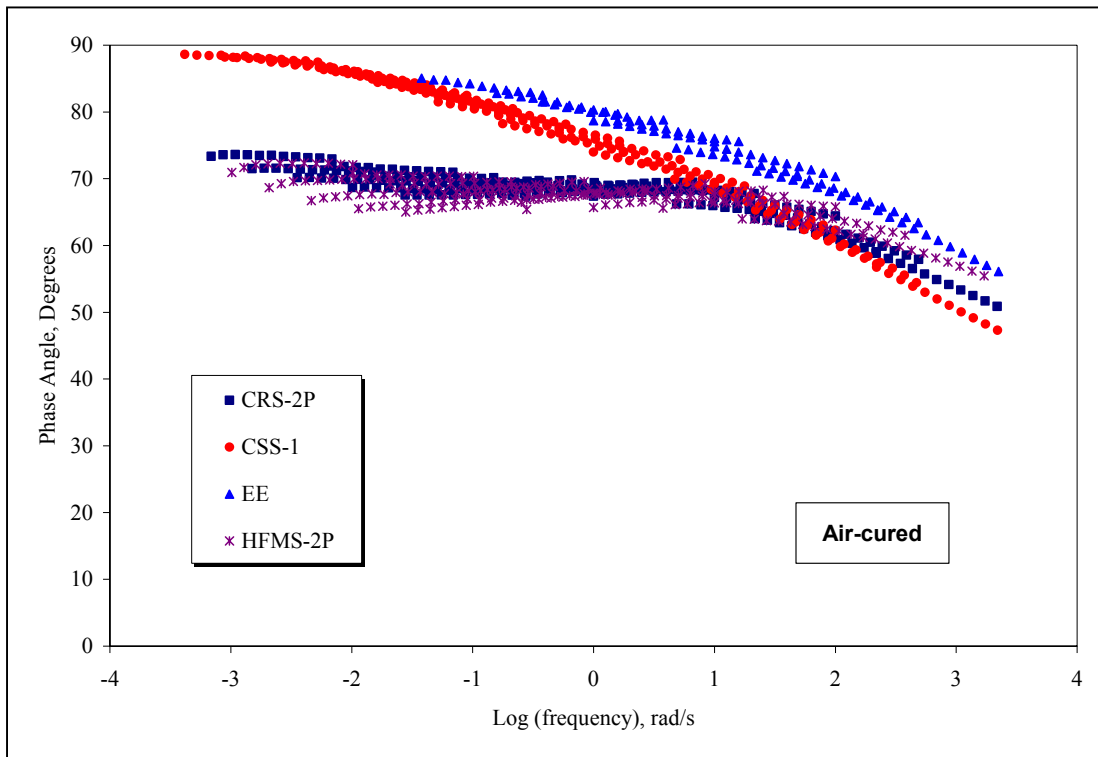


**Figure 4.16. DSR Phase Angle Master Curve, Air cured residue**

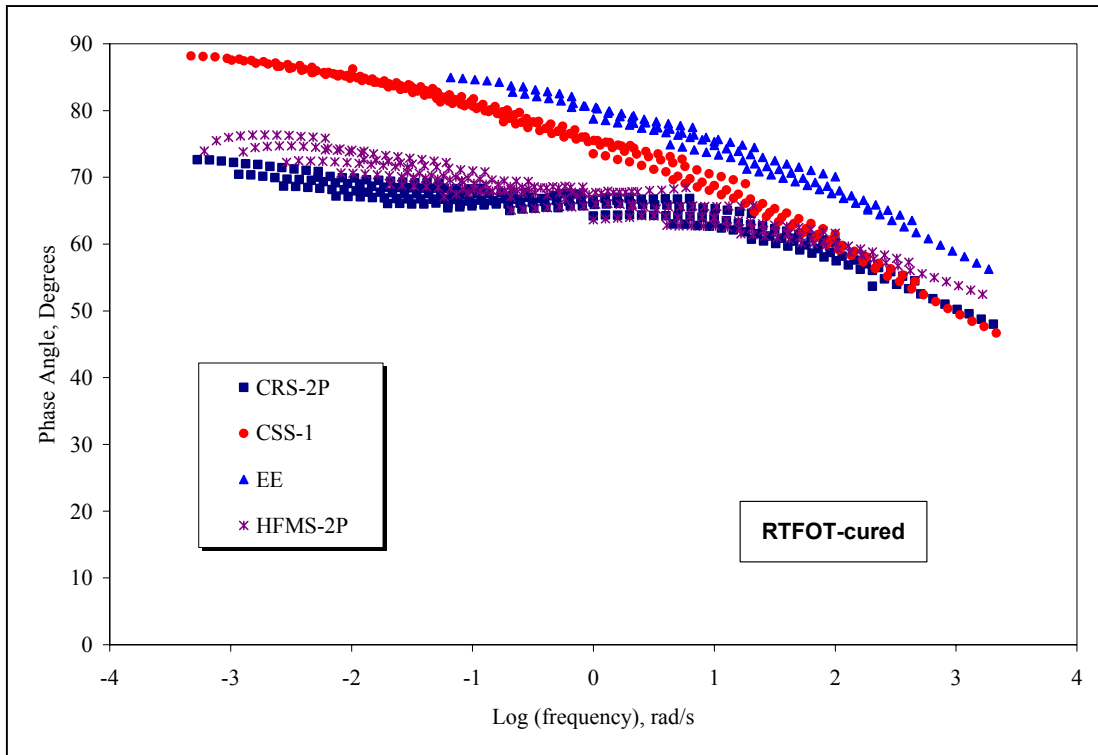


**Figure 4.17. DSR Phase Angle Master Curve, RTFOT cured residue**

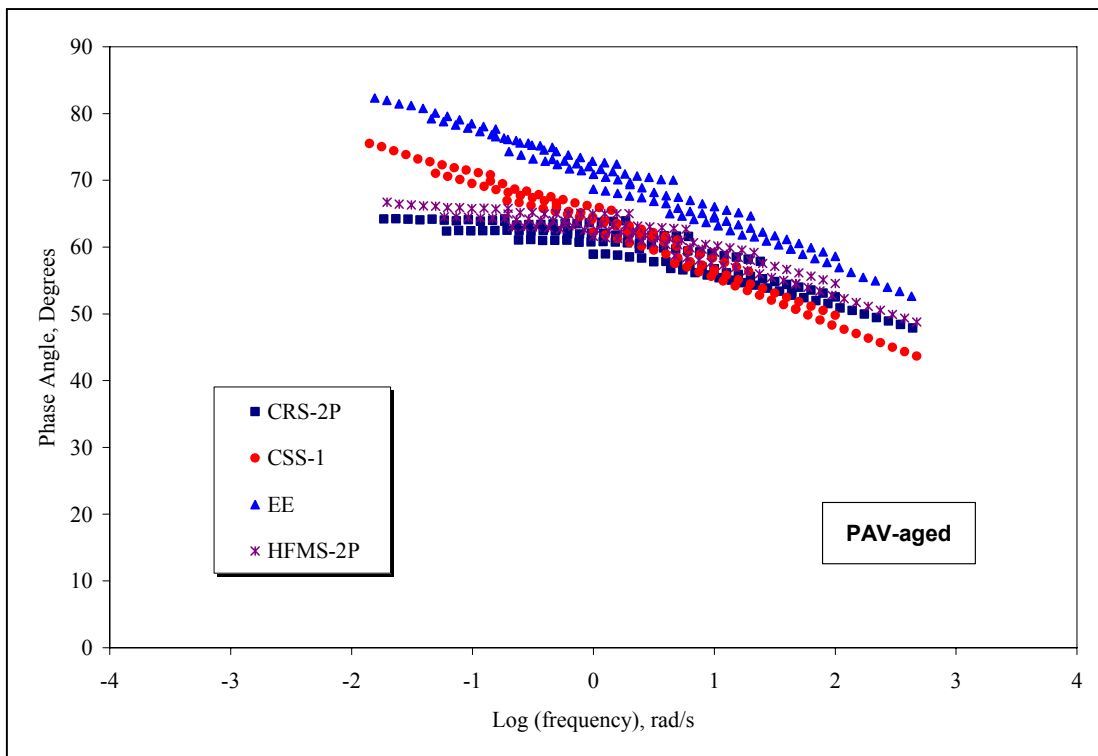


**Figure 4.18. DSR Phase Angle Master Curve, PAV aged residue**



### Temperature Master Curves at 10 rad/s

Using the time-temperature superposition principle frequencies were converted to equivalent temperature values and master curves of  $|G^*|$  as a function of temperature were generated at a fixed frequency of 10 rad/s. This is the specification frequency corresponding to traffic speeds of 60 mph (97 km/hr). Figures 4.19 to 4.21 show plots of  $|G^*|$  vs. temperature at 10 rad/s for air, RTFOT, and PAV residues, respectively. The same general trends can be seen in these plots as can be seen in the  $\log(|G^*|)$  vs.  $\log(\omega)$  master curves. The master curves are reasonably smooth with the exception of the 34°C values. It is not clear if this indicates a change in the structure of the residues or is simply a testing artifact: above this temperature, the testing was switched from the 8-mm plate to the 25-mm plate.

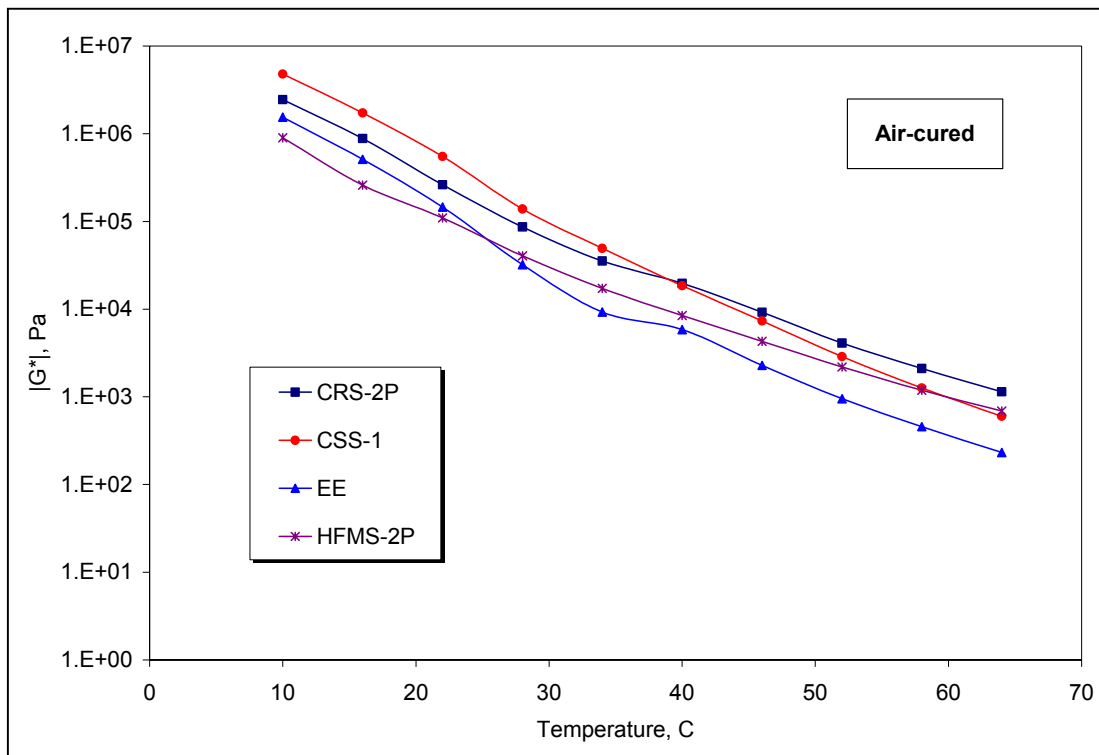


Figure 4.19.  $|G^*|$  vs. Temperature @ 10 rad/s, Air cured residue

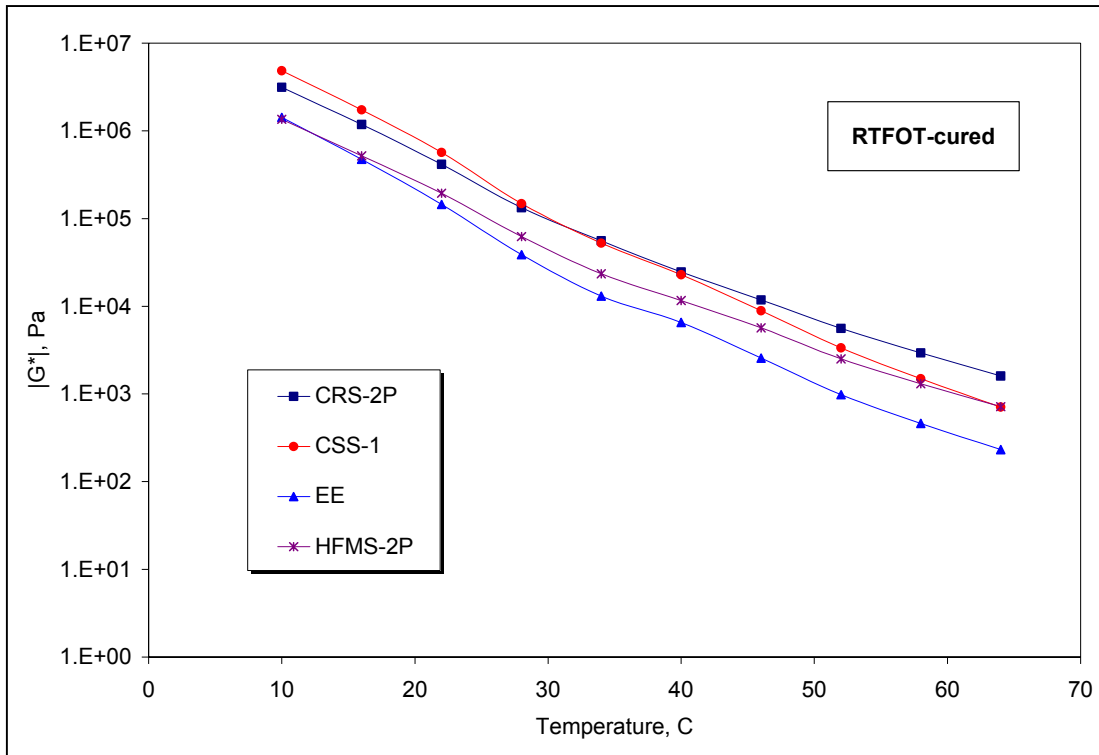


Figure 4.20.  $|G^*|$  vs. Temperature @ 10 rad/s, RTFOT cured residue

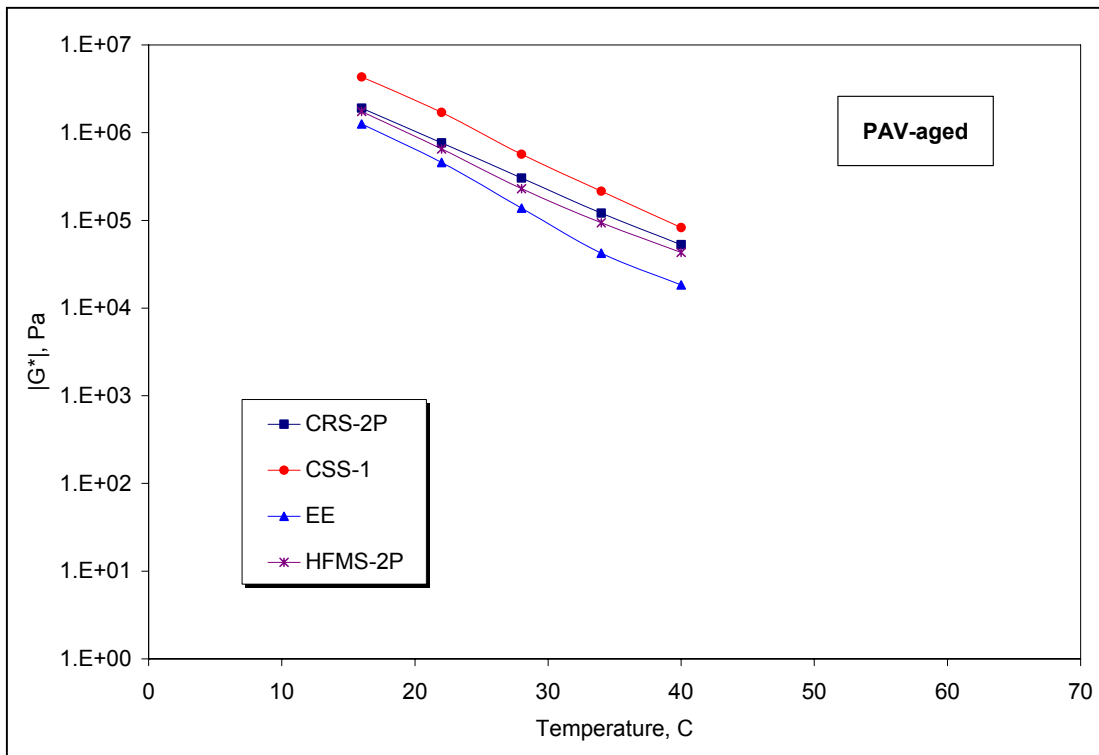


Figure 4.21.  $|G^*|$  vs. Temperature @ 10 rad/s, PAV aged residue

### Example CIR Mix Design

One of the tasks of this project included developing possible correlations between the experimental data obtained in task 3 and field performance data of CIR mixtures. Very limited field information was available during the duration of the project and as a consequence no relevant correlations could be made. As more field data becomes available correlations can be developed as part of a future project. In lieu of this comparison, a theoretical CIR mix design will be presented here. This mix design involves converting the emulsion residue DSR data to viscosity, coming up with mixture proportions such as aggregate gradation and asphalt content, predicting the dynamic modulus,  $|E^*|$ , of mixtures using these materials, and building master curves for the theoretical mixtures. These steps are explained in further detail in the following sections.

#### *Viscosity Determination*

Based on an approach described in the 2002 Design Guide, data from the DSR was used to predict binder viscosity at different temperatures. Using the data at a frequency of 10 rad/s, the viscosity of the residue is calculated by:

$$\eta = \frac{G^*}{\omega} \left( \frac{1}{\sin \delta} \right)^{4.8628} \left( \frac{1}{10^6} \right) \quad (4.3)$$

where

$\eta$  = Viscosity,  $10^6$  Poise

$G^*$  = Shear modulus, Pa

$\omega$  = Frequency, held constant at 10 rad/s

$\delta$  = phase angle, radians

A plot is then constructed of  $\log[\log(\eta)]$  vs.  $\log(T_{\text{rankine}})$ , as shown in Figure 4.22. Each of the four emulsions evaluated in this project (air-cured) are plotted here. The data can be fit with a straight line with reasonable accuracy, whereby the viscosity at any temperature can be calculated. This viscosity was later input into the empirical equation to calculate the dynamic modulus of the mixture. The viscosity values used for the prediction are shown in Table 4.10.

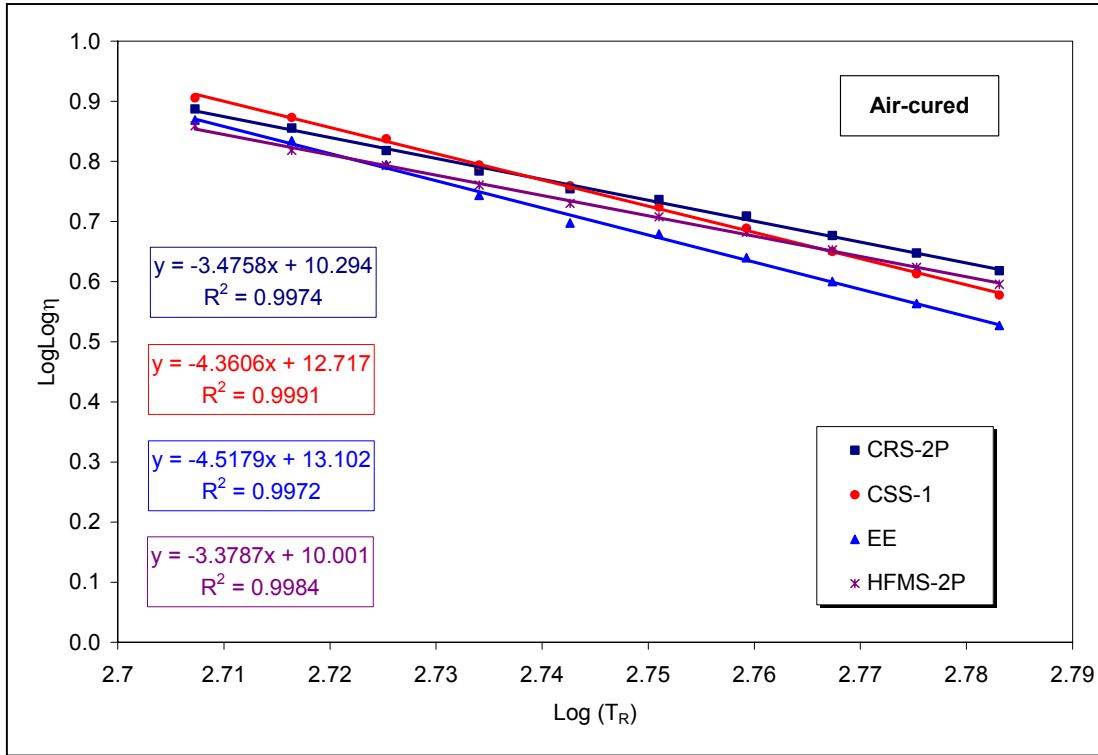


**Figure 4.22. Viscosity vs. Temperature, Air cured residues**

**Table 4.10. Calculated Viscosity Values for Emulsions**

Temperature, °C	Viscosity, 10 <sup>6</sup> Poise			
	CRS-2P	CSS-1	EE	HFMS-2P
-20	1.99E+03	1.97E+05	2.07E+04	2.68E+02
-10	7.52E+01	1.69E+03	2.18E+02	1.41E+01
4	1.77E+00	9.05E+00	1.51E+00	4.78E-01
20	6.11E-02	1.03E-01	2.23E-02	2.25E-02
40	2.48E-03	1.81E-03	5.14E-04	1.21E-03
54	4.31E-04	2.22E-04	7.36E-05	2.42E-04

*Witczak Predictive Equation*

A predictive equation was developed as part of the 2002 Design Guide. The empirical equation was developed from 2750 specimens for 205 different asphalt mixtures using regression techniques. The model for the complex dynamic modulus is as follows:

$$\log|E^*| = -1.249937 + 0.029232P_{200} - 0.001767(P_{200})^2 + 0.002841P_4 - 0.058097V_a - 0.802208 \frac{V_{beff}}{(V_{beff} + V_a)} + \frac{[3.871977 - 0.0021P_4 + 0.003958P_{38} - 0.000017(P_{38})^2 + 0.00547P_{34}]}{1 + e^{(-0.603313 - 0.313351 \log f - 0.393532 \log \eta)}} \quad (4.4)$$

where

$|E^*|$  = asphalt mix dynamic modulus, in  $10^5$  psi;

$\eta$  = binder viscosity, in  $10^6$  poise;

$f$  = load frequency, in Hz;

$V_a$  = percent air voids in the mix, by volume;

$V_{\text{beff}}$  = percent effective bitumen content, by volume;

$P_{34}$  = percent retained on  $\frac{3}{4}$ -in. (19-mm) sieve, by total aggregate weight (cumulative);

$P_{38}$  = percent retained on  $\frac{3}{8}$ -in. (9-mm) sieve, by total aggregate weight (cumulative);

$P_4$  = percent retained on #4 (4.75-mm) sieve, by total aggregate weight (cumulative); and

$P_{200}$  = percent passing #200 (0.075-mm) sieve, by total aggregate weight.

The parameters used for this study in equation 4.4 were based on those used by Salomon and Newcomb [9]. They are presented in Table 4.11.

**Table 4.11. CIR Mix Design Parameters**

Parameter	Description	Value	Unit	Comment
$V_a$	% air voids in mix	7.0	%	by volume
$V_{\text{b-eff}}$	% effective binder content	12.45	%	by volume
$p_{34}$	% <b>retained</b> on $\frac{3}{4}$ " sieve	0	%	by total aggregate weight (cumulative)
$p_{38}$	% <b>retained</b> on $\frac{3}{8}$ " sieve	10	%	by total aggregate weight (cumulative)
$p_4$	% <b>retained</b> on #4 sieve	20	%	by total aggregate weight (cumulative)
$p_{200}$	% <b>passing</b> #200 sieve	7	%	by total aggregate weight

The predictive equation was used to calculate the dynamic modulus of the theoretical mixture using the parameters in Tables 4.10 and 4.11 over a range of temperatures and frequencies with each of the four emulsions. The predicted modulus values are shown in Tables 4.12 to 4.15.

**Table 4.12. Predicted Dynamic Modulus, CRS-2P**

Frequency, Hz	Predicted Dynamic Modulus in GPa					
	Temperature, °C					
	-20	-10	4	20	40	54
25	18.097	10.944	4.565	1.565	0.478	0.246
10	16.478	9.482	3.698	1.206	0.362	0.188
1	12.446	6.250	2.064	0.609	0.183	0.099
0.1	8.740	3.790	1.080	0.304	0.096	0.055
0.01	5.660	2.122	0.543	0.154	0.054	0.034

**Table 4.13. Predicted Dynamic Modulus, CSS-1**

Frequency, Hz	Predicted Dynamic Modulus in GPa					
	Temperature, °C					
	-20	-10	4	20	40	54
25	27.209	17.734	6.971	1.876	0.424	0.193
10	25.949	16.113	5.817	1.454	0.321	0.148
1	22.436	12.097	3.482	0.742	0.163	0.079
0.1	18.533	8.435	1.928	0.370	0.087	0.046
0.01	14.467	5.422	1.004	0.186	0.049	0.029

**Table 4.14. Predicted Dynamic Modulus, EE**

Frequency, Hz	Predicted Dynamic Modulus in GPa					
	Temperature, °C					
	-20	-10	4	20	40	54
25	23.061	13.202	4.369	1.089	0.263	0.130
10	21.570	11.642	3.530	0.831	0.201	0.101
1	17.606	8.044	1.958	0.415	0.105	0.057
0.1	13.545	5.120	1.020	0.208	0.058	0.034
0.01	9.715	3.000	0.512	0.109	0.035	0.023

**Table 4.15. Predicted Dynamic Modulus, HFMS-2P**

Frequency, Hz	Predicted Dynamic Modulus in GPa					
	Temperature, °C					
	-20	-10	4	20	40	54
25	13.652	7.729	3.100	1.094	0.364	0.199
10	12.078	6.502	2.457	0.835	0.276	0.153
1	8.419	3.971	1.307	0.417	0.141	0.082
0.1	5.410	2.238	0.663	0.209	0.076	0.047
0.01	3.199	1.180	0.330	0.109	0.044	0.029

### *Mixture Master Curves*

The dynamic modulus and phase angle of asphalt mixtures, similar to asphalt binders, can be shifted along the frequency axis to form master curves at a desired reference temperature or frequency. This procedure assumes that asphalt mixtures are thermorheologically simple materials and the time-temperature superposition principle is applicable.

A new method of constructing the master curve for asphalt mixtures was developed by Pellinen [13]. In this study, master curves were constructed fitting a sigmoidal function to the measured compressive dynamic modulus test data using non-linear least squares regression techniques. The shift can be done by solving the shift factors simultaneously with the coefficients of the sigmoidal function. The sigmoidal function is defined by the following equation:

$$\log|E^*| = \delta + \frac{\alpha}{1 + e^{\beta - \gamma(\log(f_r) + s_T)}} \quad (4.5)$$

where

$\log|E^*|$  = log of dynamic modulus (GPa),

$\delta$  = minimum modulus value,

$f_r$  = reduced frequency,

$\alpha$  = span of modulus values,

$s_T$  = shift factor according to temperature, and

$\beta, \gamma$  = shape parameters.

This method was used to construct master curves using the predicted dynamic modulus values. The reference temperature for all mixtures was 20°C. The commercial computer program SigmaStat was used to fit the master curve for each set of data. Table 4.16 shows the fitted model parameters for each mixture. The master curve of  $|E^*|$  vs. frequency is shown in Figure 4.23. This curve shows a similar trend to the binder master curves, which would be expected. CSS-1 has the stiffest mixture over the entire range of frequencies, followed by CRS-2P. The curves for EE and HFMS-2P fall directly on top of each other. For this mix design, they would result in similar modulus values. This results should be interpreted with caution because the

design guide regression equation was developed based on HMA data and did not include CIR mixtures.

**Table 4.16. Mixture Model Parameters**

	CRS-2P	CSS-1	EE	HFMS-2P
$\alpha$	3.8705	3.8675	3.8684	3.866
$\delta$	-2.2723	-2.2696	-2.2703	-2.2695
$\beta$	-0.1263	-0.214	0.0472	0.0448
$\gamma$	-0.313	-0.3133	-0.3133	-0.3136
s (-20)	5.6688	7.8876	7.4936	5.1181
s (-10)	3.8817	5.2947	5.0108	3.5115
s (4)	1.8357	2.4427	2.3009	1.6643
s (20)	0	0	0	0
s (40)	-1.7478	-2.2037	-2.0552	-1.5941
s (54)	-2.7037	-3.3512	-3.1166	-2.4717

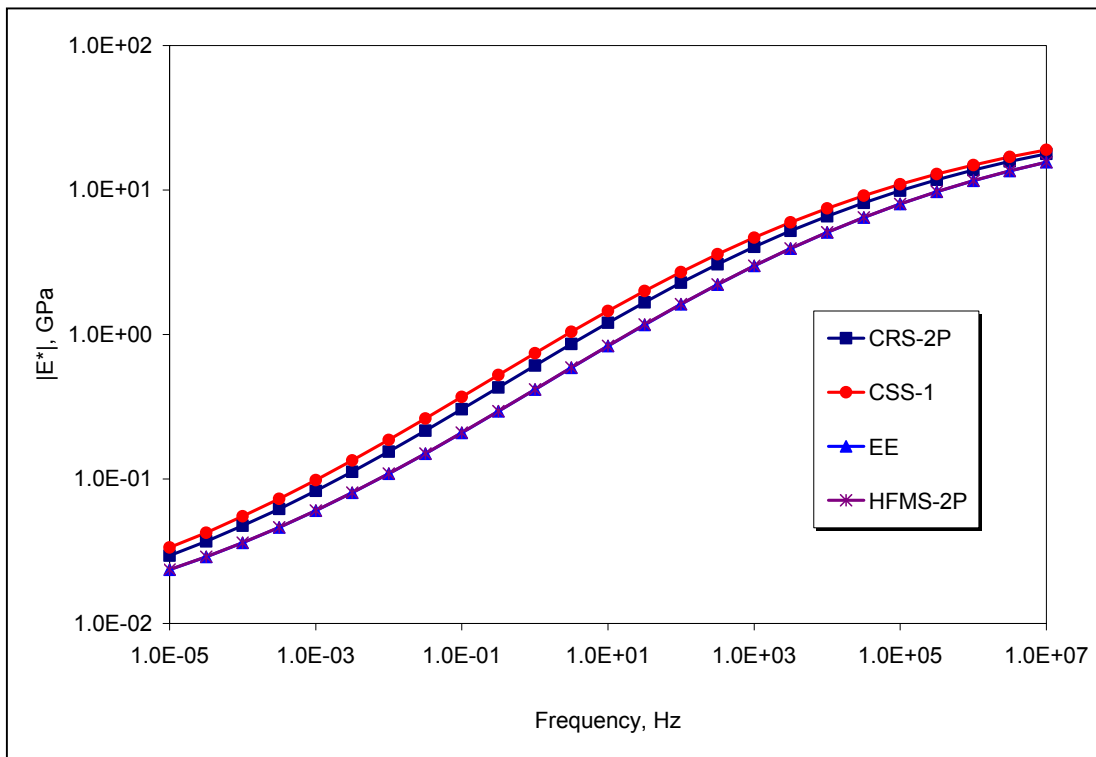


**Figure 4.23. Mixture Master Curves ( $|E^*|$  vs. Frequency) from Witczak Equation**



Using time-temperature superposition, master curves of dynamic modulus vs. temperature were constructed for a reference frequency of 10 Hz. These curves are shown in Figure 4.24.

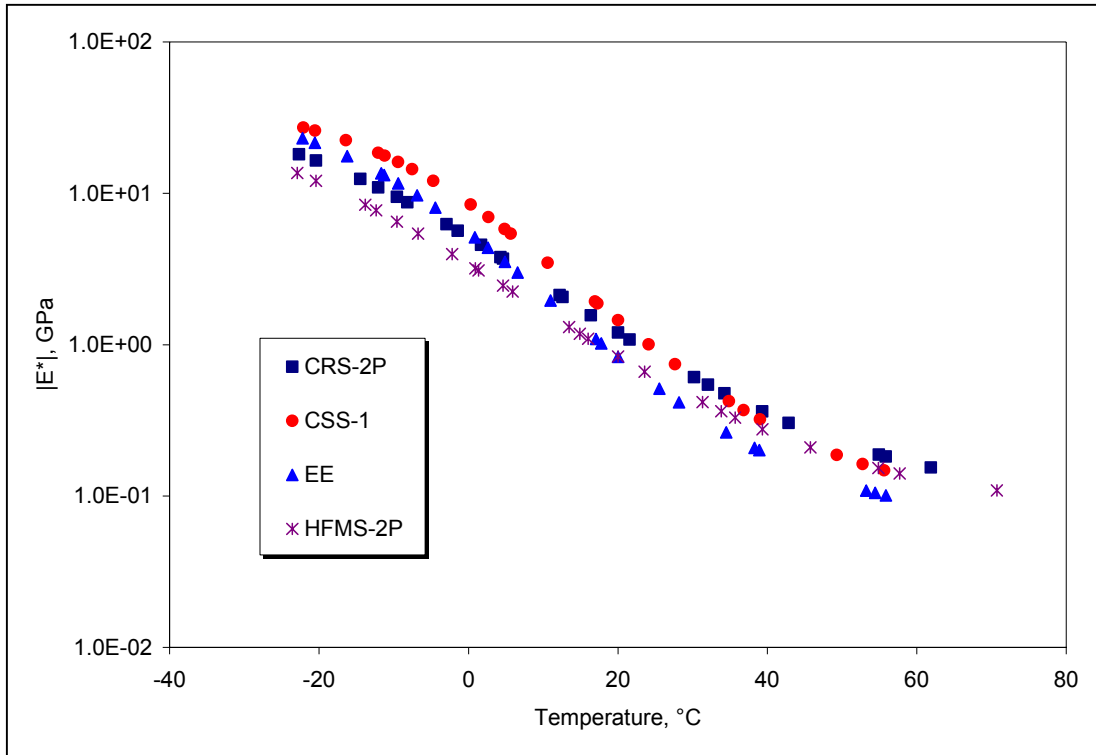


**Figure 4.24. Mixture Master Curves ( $|E^*|$  vs. Temperature) from Witczak Equation**

For comparison, a master curve was also constructed from a previous project. Cell 34 from MnROAD was chosen to compare against the four emulsion mix designs. It contained a different aggregate gradation, different binder content, and a PG 58-34 asphalt binder that had different viscosity values than the theoretical mix designs presented here. The master curve was constructed for this mixture, and added to the plots shown in Figures 4.23 and 4.24 above. These additional plots are shown in Figures 4.25 and 4.26. The plots clearly show that the conventional dense-graded Superpave mix (Cell 34) is significantly stiffer than the mixtures containing the asphalt emulsions.

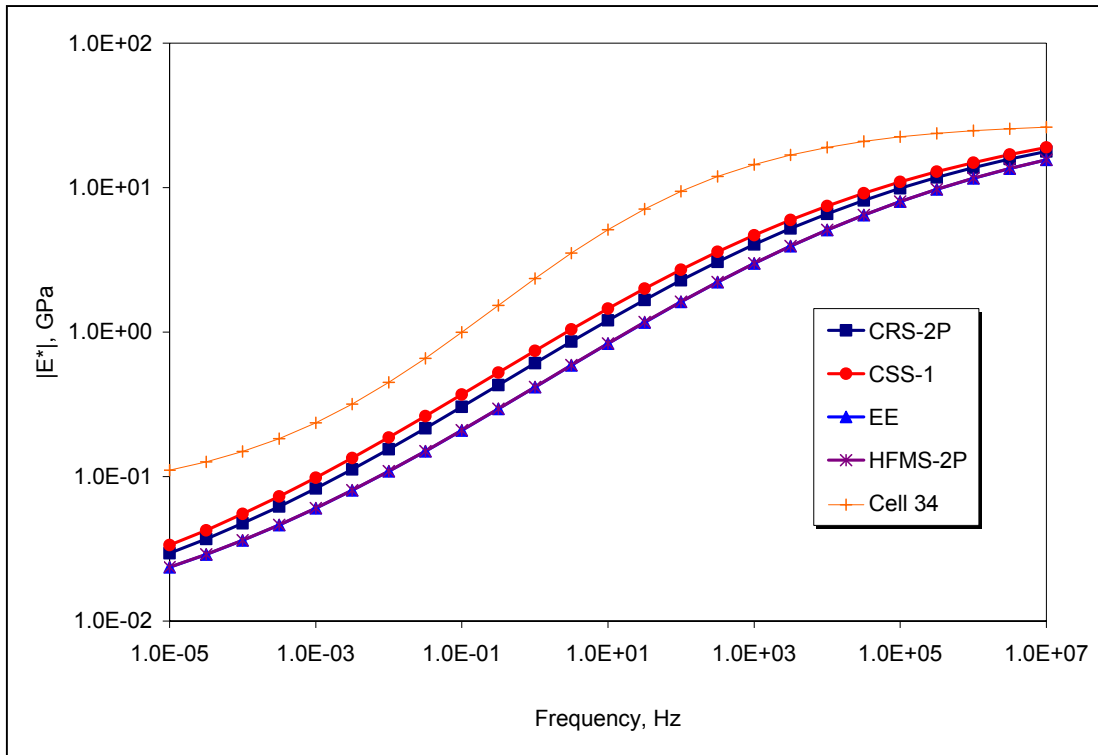


Figure 4.25.  $|E^*|$  vs. Frequency, Emulsions and Cell 34

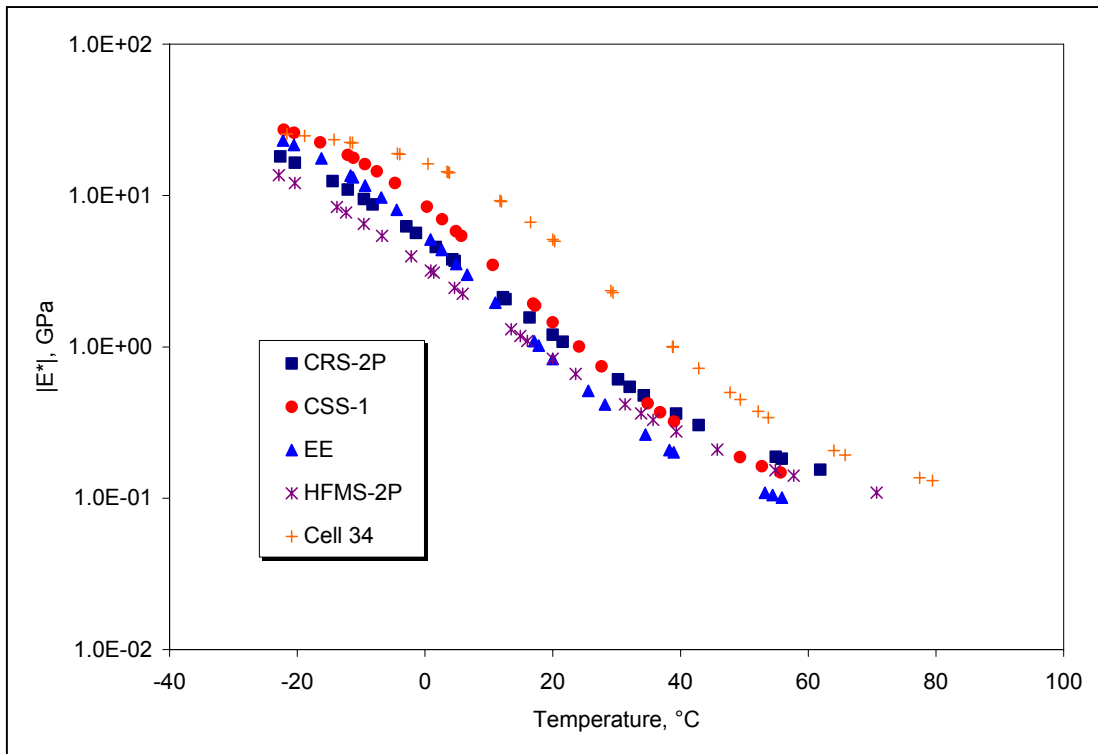


Figure 4.26.  $|E^*|$  vs. Temperature, Emulsions and Cell 34

# CHAPTER 5

## RESULTS AND RECOMMENDATIONS

### Results

The goal of this project was to develop a system to better characterize asphalt emulsions commonly used in cold in-place recycling (CIR) mixtures. Four different asphalt emulsions, three of which are used in CIR applications and one is used surface treatment applications included for comparison purposes, were cured and the residues tested in the Superpave binder test apparatus. The results obtained in this research are as follows:

1. The asphalt emulsions were cured by two different methods: air-cured and RTFOT-cured. The RTFOT-cured specimens had higher limiting temperatures (high temperature criterion) than the air-cured specimens, with differences ranging between 0.7°C for EE to 3.4°C for CRS-2P, indicating that the RTFOT curing procedure resulted in stiffer residues. A similar but less pronounced trend is observed for both the BBR and the DT test results, with the exception of EE emulsion residue for which the limiting temperatures were slightly higher for the air-cured specimens.
2. Based on the laboratory test results and the MP1 criteria for RTFOT and PAV conditions “PG” grades, similar to the conventional binders PG grades, were determined for the emulsion residues investigated.
3. MP1a analysis showed that the critical cracking temperature,  $T_{cr}$ , obtained by the intersection of thermal stress and strength curves was substantially higher than the limiting temperatures obtained from MP1. This trend seems to be reasonably explained by the fact that the DT strength data for these emulsions (approximately 1 MPa) is significantly lower than strength data for typical asphalt binders (approximately 2-7 MPa). Also note that for all four emulsions the DT limiting values according to MP1 specification, were always higher than the BBR S(60s) and m(60s) limiting temperatures indicating that the failure strains were also small compared to conventional binders.
4. The CAM model was successfully used to generate smooth master curves of  $|G^*|$  for each of the residues. One exception was the data obtained at 34°C for EE air that showed a drop in modulus at the higher end of the frequency sweep.

5. Master curves were also constructed for phase angle vs.  $\log(\omega)$ . The phase angle master curves were less smooth indicating most probably the presence of small phase transitions or thixotropy effects, especially in the polymer modified samples. CRS-2P and HFMS-2P also showed a pronounced plateau in phase angle, which is similar to the trend observed in conventional polymer-modified binders.
6. A theoretical CIR mix design was presented using viscosity values calculated from DSR test results and volumetric data available from a previous MNDOT research report. An empirical equation developed in the 2002 Design Guide was used to predict the complex dynamic modulus of the CIR mixture. A sigmoidal function was used to fit the master curves of the mix data. A comparison to a conventional dense-graded Superpave mixture showed that the Superpave mixture was significantly stiffer than the mixtures containing asphalt emulsions over the entire range of frequencies and temperatures.

## **Recommendations**

The results presented in this study should be viewed as a first step in the development of a comprehensive performance base CIR material selection specification. The research performed in this study demonstrates the possibility of adapting the current PG test protocols and analyses to asphalt emulsion characterization. This approach offers the advantage of comparing conventional asphalt binders and asphalt emulsions based on a similar set of test protocols. However, extensive well-documented field data, which was not available at the time of this research project, is required to develop meaningful correlations between the experimental data and the actual performance of CIR mixtures. In addition, a study of the interaction between the RAP and the asphalt emulsion should be performed to better understand the role of the RAP binder in the CIR mixture performance as well as the asphalt emulsion mixing and setting characteristics. With respect to the pavement design aspect of CIR, extensive experimental data performed on laboratory prepared CIR mixtures will be required to validate and eventually modify the predictive equation developed as part of the 2002 Design Guide, that was used in chapter 4 to predict the complex dynamic modulus of a typical CIR mixture.

## REFERENCES

1. *Asphalt Institute*, MS-19, Chapter 4, Testing Asphalt Emulsion.
2. Takamura, K., "Comparison of Emulsion Residues Recovered by Forced Airflow and RTFO Drying," ISSA/AEMA Proceedings, March 12-15, 2000, pp. 1-17.
3. King, G. et al, "SHRP Test Evaluation of High Float and Polymer Modified Bitumen Emulsion Residues," Koch Materials Laboratory, Terre Haute, IN.
4. Barcena, R., Epps, A., and D. Hazlett, "A Performance-Graded Binder Specification for Surface Treatments," Submitted for presentation and publication at the 81<sup>st</sup> Annual Meeting of the Transportation Research Board, Washington, D.C., January 2002.
5. Salomon, D., "Analysis of Asphalt Emulsions by Rotational Viscometry," I. ISSA/AEMA Proceedings, March 12-15, 2000, pp. 71-80.
6. Deneuvillers, C., et al, "Contribution to the Study of the Relationship between Characteristics and Performances of Bitumen Emulsions," 2<sup>nd</sup> Eurasphalt & Eurobitume Congress, Barcelona 2000, Book 1, pp. 195-202.
7. Le Bec, et al, "Formulation of Cold Mixes: Accelerated Curing in the Laboratory," 2<sup>nd</sup> Eurasphalt & Eurobitume Congress, Barcelona 2000, Book 1, pp. 1-7.
8. Leseur, D., "Predicting the In-Place Compacity of Cold Mixes," 2<sup>nd</sup> Eurasphalt & Eurobitume Congress, Barcelona 2000, Book 1, pp. 315-325; "Emulsion/Aggregate Interactions through Water Analysis," 2<sup>nd</sup> Eurasphalt & Eurobitume Congress, Barcelona 2000, Book 1, pp. 326-334.
9. Salomon, A. and D. E. Newcomb, "Cold In-Place Recycling Literature Review and Preliminary Mixture Design Procedure," Minnesota Department of Transportation, Final Report 2000-21, 2000.
10. Brayton, T. E., et al, "Development of Performance-Based Mix Design for Cold In-Place Recycling of Asphalt Mixtures," Transportation Research Board Annual Meeting, 2001.
11. Croteau, J-M., et al, "Uses of Emulsion Mixes to Mitigate the Effect of Subgrade Movements," ISSA/AEMA Proceedings, March 12-15, 2000, pp. 143-160.

12. A. Basu, "An Evaluation of the Time-Temperature Equivalence Factor and of the Physical Hardening Effects on Low-Temperature Asphalt Binder Specifications," M.S. Thesis, University of Minnesota, 2002.
13. Pellinen, T. K., and M. W. Witzak, "Stress Dependent Master Curve Construction for Dynamic (Complex) Modulus," *Journal of the Association of Asphalt Paving Technologists*, Vol. 71, 2002.